DIPLOMA THESIS

Design of the Thermal Control System for Compass-1

Sylwia Czernik
University of Applied Sciences Aachen
Germany

August 2004

This work is done within the student satellite project
"Compass-1"
at the University of Applied Sciences Aachen, Germany

Design of the Thermal Control System for Compass-1

Sylwia Czernik

Supervision:
Prof. Dr. rer. nat. Hans-Joachim Blome
Prof. Dr.-Ing. Wilfried Ley

Abstract

In October 2003, a satellite project was initiated at the University of Applied Sciences, Aachen, Germany in order to give undergraduate students the rare opportunity to experience all the challenging aspects associated with satellite design, manufacture and operation. The spacecraft, labeled “Compass-1”, follows the design concept of a “CubeSat”, a standard picosatellite design, jointly developed by California Polytechnic State University San Luis Obispo and Stanford University Space Systems Development Lab. The CubeSat concept defines a cubic structural bus of dimensions 10x10x10cm³ and a total mass of not more than 1kg. Compass-1 is designed for a circular, (near) Sun-synchronous Low Earth Orbit (LEO) with an altitude of 600km and an inclination of 98°. Its designed operation time is 6 month.

To ensure a successful flight, it is necessary within the scope of the project to design an adequate Thermal Control System (TCS). This work summarizes the thermal design and thermal analysis of Compass-1.

Contents

List of Figures

List of Tables

List of Symbols

A	Surface area
A_P	projected surface area that is exposed to Earth-shine/sunshine
c	speed of light
c_w	specific heat
F_{ij}	View factor
H	Altitude
i	Inclination
I_S	Solar radiation
I_E	Earth infrared radiation
k	Boltzmann constant
m	mass
R_E	Radius of Earth
T	Temperature
t_E	Eclipse duration
t_u	Orbital duration

Greek

α	Absorptivity
β	Beta angle
ε	Emissivity
λ	Wavelength
σ	Stefan-Boltzmann Constant
ρ	Density
ρ'	angular radius of the Earth
γ	Gravity constant

List of Abbreviations

Al	Aluminum
Bp	Black paint
CDHS	Command and Data Handling System
EPS	Electrical Power System
FEM	Finite element model
IR	Infrared radiation
LEO	Low Earth Orbit
MLI	Multi Layered Insulation
RSM	Radiosity Solver Method
Sc	Solar cell
SSP	Sub Solar Point
TCS	Thermal Control System
WHC	Worst hot case
WCC	Worst cold case

Nomenclature

Background temperature	$T_{space} = 3[K]$
Earth Radius	$R_E = 6370km$
IR Radiation	$I_E = 230\left[\frac{W}{m^2}\right]$
Albedo	$I_a = 470\left[\frac{W}{m^2}\right]$
Heat flux Sun	$I_S = 1370\left[\frac{W}{m^2}\right]$
Altitude of Compass-1	$H = 600[km]$
total surface area of the spacecraft	$A_T = 6 \cdot 0.1^2[m^2]$
Gravity constant	$\gamma = 6{,}67 \cdot 10^{-11}\left[\frac{Nm^2}{kg^2}\right]$
Stefan-Boltzmann-Constant σ	$\sigma = 5.67 \cdot 10^{-8}\left[\frac{W}{m^2K^4}\right]$
Speed of light	$c \approx 3 \cdot 10^8 \frac{m}{s}$
Boltzmann constant	$k = 1.380 \cdot 10^{-23}\left[\frac{Ws}{K}\right]$

Introduction

Unlike terrestrial or airborne vehicles, spacecrafts in general and satellites in particular are subject to an extreme thermal environment. Body temperatures ranging from -100°C to +100°C are not uncommon in astronautical engineering applications. Sometimes these extreme temperatures are present at the same time at different locations of the spacecraft. Fairly straightforward analytical and numerical methods are available to compute the thermal behavior for a given geometrical satellite structure in LEO. The thermal control engineer must derive essential conclusions from these results and design thermal management solutions that satisfy the operational temperature limits of all components installed on the spacecraft. Numerical simulation is the most important tool for the thermal control engineer. Considerable effort must be spent in determining the thermal behavior of a body. The derived system solutions often seem trivial on first sight but in fact they are highly optimized solutions emerging from comprehensive and sophisticated design preparations.

1. Thermal Environment

Compass-1 will be exposed to physical conditions and terms, which are different from the conditions on Earth.

The Sun's radiation is the greatest source of energy incident on most spacecrafts. The emitted radiation from the Sun is constant within a fraction of 1% at all times. However, due to the Earth's elliptical orbit, the intensity of the Sun's radiation reaching the LEO varies by approximately ±3,5% depending on the Earth's distance from to the Sun. In summer (northern hemisphere) the intensity is at a minimum of 1372W/m^2 and at winter solstice the maximum of 1417W/m^2 is reached. The value of the solar constant varies, because of changes in the average distance Earth-Sun. The eccentricity expresses to what extent the Earth's orbit around the Sun differs from a circle. The orbit is somewhat elliptical, and a higher eccentricity corresponds to a more elliptical orbit. The solar constant can be calculated with [R1]:

$$I_{\perp Earth} = I_E \left[1 + 0.033 \cdot \cos\left(360° \cdot \frac{n}{365} \right) \right] \qquad (1)$$

where:

$I_{E\max} = 1417 \, W/m^2$
$I_{E\min} = 1327 \, W/m^2$
$I_E =$ currently solar constant
n = day number of the year

The radiation of the Sun that is reflected off of a planet or its atmosphere is known as Albedo. The Earth's Albedo is usually expressed as a percentage of incident sunlight that is reflected back in to space and is highly variable. As a first approximation one can assume a value of about 34%. However, reflectivity is generally greater over continental regions as compared to oceanic regions and generally increases with decreasing elevation angles and increasing cloud coverage.

The Earth does not only reflect the radiation of the Sun, but also emits long-wave IR radiation due to its temperature. The Earth, as well as a satellite, achieves thermal equilibrium by balancing the energy received (absorbed) from the Sun with the energy re-emitted as long-wavelength IR radiation into space. This balance is maintained fairly well on a global annual average basis. As a first approximation one can use a value of around $237 \pm 21 W/m^2$ emitted from the earth's surface.

At satellite altitudes the background of the space is black. Radiation (gamma, X, ultraviolet, visible, infrared and radio) from deep space represents a very small amount of energy.
The temperature background for a satellite in space is 2.7K and the pressure surrounding is very close to total vacuum.

This radiative environment causes extreme temperature variations in the satellite's outer skin. Thus the outside layers of insulating blankets can reach temperatures of 100°C when turned towards to the Sun and drop to -100°C when in the shadow of the satellite or Earth.

Radiation balance of Compass1 in LEO

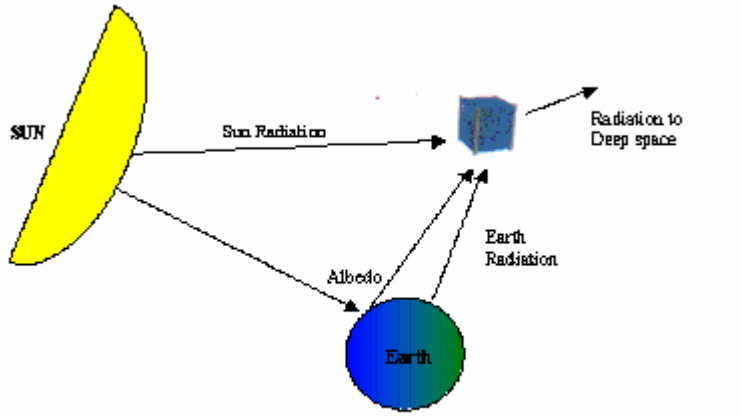

Figure 1-1 Space environment for Compass-1 in LEO

The temperature requirements for each subsystem are shown in *Table 1-1:*

Components	Operating Temperature Range [°C]
Camera	-10…+70
Electronics	-40 +85
Battery	+5…+20
Solar cells	-100…+100
Structure	-45…+65

Table 1-1 Operating temperature limits

The following *Table 1-2* contains the constraints for the thermal control system design:

Constraints
- Peak power < 1W - Average power < 80mW - Mass below 30g

Table 1-2 TCS constraints

Compass-1 in space interacts with its environment by radiation. This exchange of energy by means is: solar radiation, Albedo, Earth infrared radiation and radiation from the spacecraft to deep space. The purpose of thermal design is to maintain the temperature of all spacecraft components within desired temperature limits using the basic energy balance requirement:

$$m \cdot c_w \frac{dT}{dt} = \dot{Q}_{in} - \dot{Q}_{out} \quad (2)$$

1.1. Space environment

The space environment is a complex, orbit depend phenomenon. LEOs are orbits at a height of less than 2,000km above the Earth' surface. The space environment in LEO contains many concerns that need to be considered in the design of a space-craft. The most important features of the space environment are: vacuum, radiation and residual atmosphere.

1.1.1 The atmosphere

In LEO, above 600km, the density and the pressure are very low. *Figure 1-2* provides the atmospheric pressure depended on the altitude. It can be seen, that beginning from an altitude 500km the pressure is nearly $10^{-14}\ kg/m^3$. It means that vacuum can be assumed.

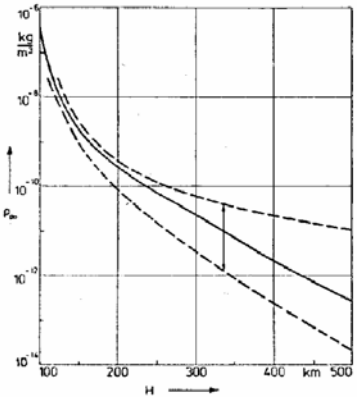

Figure 1-2 Atmosphere pressure as a function of altitude

Atomic oxygen is another important part of the atmosphere's effect in LEO. Atomic oxygen results from the interaction of solar radiation with oxygen. The perturbations in orbital period are very slight and therefore they can be neglected. *Figure 2-2* shows the air density as a function of altitude.

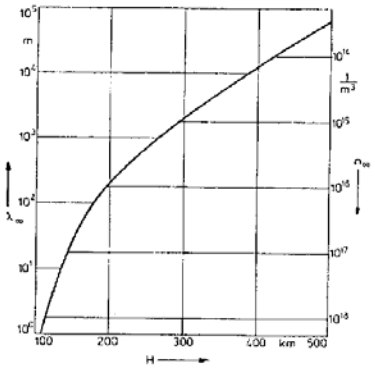

Figure 1-3 Density as a function of altitude

1.1.2 Spectrum of solar radiation

Solar intensity varies as a function of wavelength. The energy distribution is approximately 7% ultraviolet, 46% visible and 47% near infrared with the total integrated energy being equal to the $1327W/mm^2$ to $1417W/mm^2$ values mentioned above.

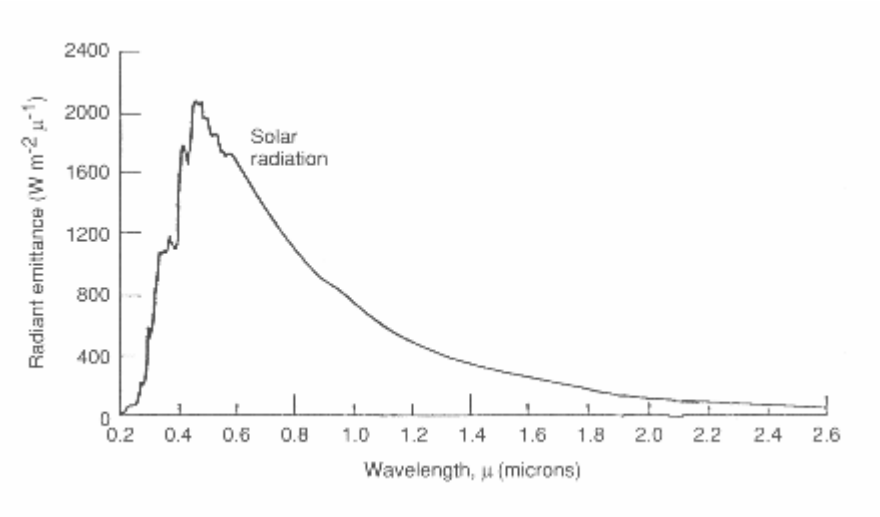

Figure 1-4 Spectral distribution of Sun radiation in LEO

Black body

An ideal black body is a theoretical object that absorbs all the incident energy and emits all of its thermal energy. Planck's law gives the spectral power distribution over the wave-length for a black body and the Stefan-Boltzmann law expresses the total power radiated. Black body radiation is the radiation emitted by a perfect black body object. The radiated energy density ρ (energy per unit volume per unit wavelength range) depends on the wavelength and is given by Planck's law.

1.2. Orbital parameters

Compass-1 is designed for a circular, near Sun synchronous LEO at an altitude of 600 km and an inclination of 98°. The Sun synchronous orbit has the characteristic of maintaining the orbit plane at a nearly fixed angle relative to the Sun. The result of this is that, on every orbit, the satellite passes over points on the Earth that has the same local time. Because the Earth rotates beneath the orbit, the satellite sees a different swath of the Earth's surface on each revolution and can cover nearly the entire globe over the course of a day.

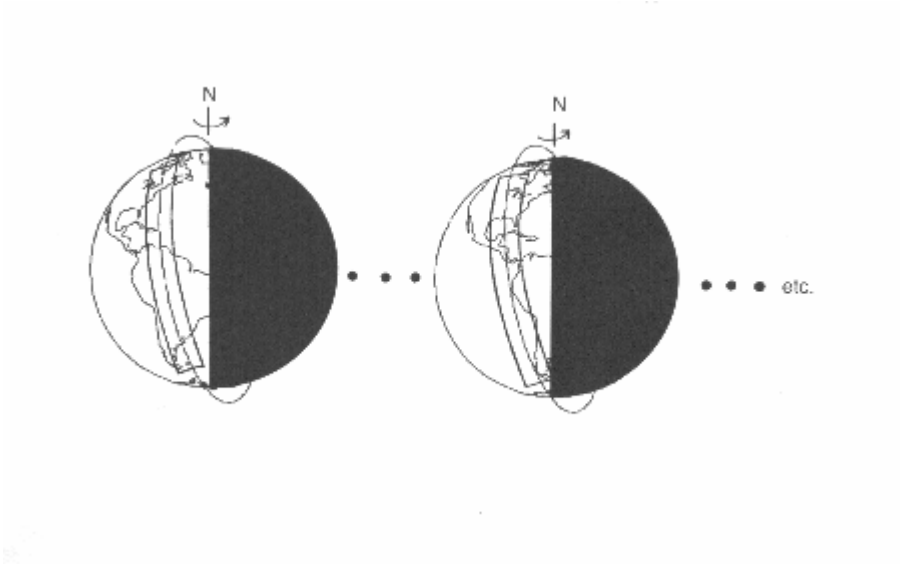

Figure 1-5 Sun synchronous orbit

In LEO, there is another parameter, known as the orbit beta angle β, which is very useful in visualizing the orbital thermal environment, particularly for the LEOs. The beta angle is defined as the minimum angle between the orbit plane and the solar vector and can vary between –90° and +90°, as illustrated in *Figure1-6*. The beta angle is defined mathematically as:

$$\beta = \arcsin(\cos\delta_s \sin i \cdot \sin(\alpha - \alpha_s) + \sin\delta_s \cos i) \qquad (3)$$

where

δ_s = declination of the Sun
i = orbit inclination
α = right ascension of the ascending node
α_s = right ascension of the Sun
β = beta angle

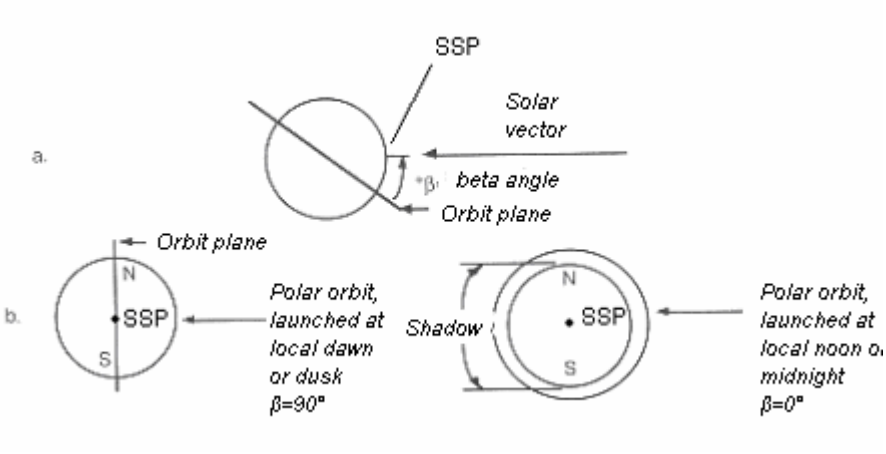

Figure 1-6 Orbital beta angle

As viewed from the Sun, a β=0° orbit would appear edgewise as a Sub-Solar Point (SSP), as shown in *Figure 1-6.b*. A satellite in such an orbit would pass over the Sub-Solar Point on the Earth (the point on Earth where the Sun is directly overhead). That is where Albedo loads are the highest, but it would also have the longest eclipse time due to shadowing by the full diameter of the Earth. As the β angle increases, the satellite passes over areas of the Earth further from the Sub-Solar Point, thereby reducing Albedo loads; however, the satellite will also be subjected to the Sun for a larger percentage of each orbit due to decreasing eclipse times. At one position, which varies depending on the altitude of the orbit, eclipse time drops to zero. At a beta angle of 90° a circular orbit appears as a circle as seen from the Sun there are no eclipses independent of altitude, and Albedo loads are near zero. It should also be noted here that the beta angle is often expressed as positive or negative positive if the satellite appears to be going counter-clockwise around on its orbit as seen from the Sun, negative if clockwise moving. [R2]

The eclipse fraction for a circular orbit can be calculated from the following equation:

$$t_E = \frac{1}{180°}\cos^{-1}\left(\frac{(h^2 + 2RH)^{0.5}}{(R+H)\cos\beta}\right) \qquad \text{if } |\beta| < \beta^* \qquad (4)$$

where

R_E = Earth's radius
H = orbit altitude
β = orbit beta angle
β*= beta angle at which eclipses begin

β* may be calculated using:

$$\beta^* = \sin^{-1}\left(\frac{R_E}{R_E + H}\right) \tag{5}$$

Equations (3) and (4) assume that the Earth's shadow is cylindrical, which is valid for low orbits where there is no appreciable difference between the umbra and penumbral regions of total and partial eclipsing, respectively. In this case the orbit plane is parallel to the Sun vector (*Figure 1-7*).

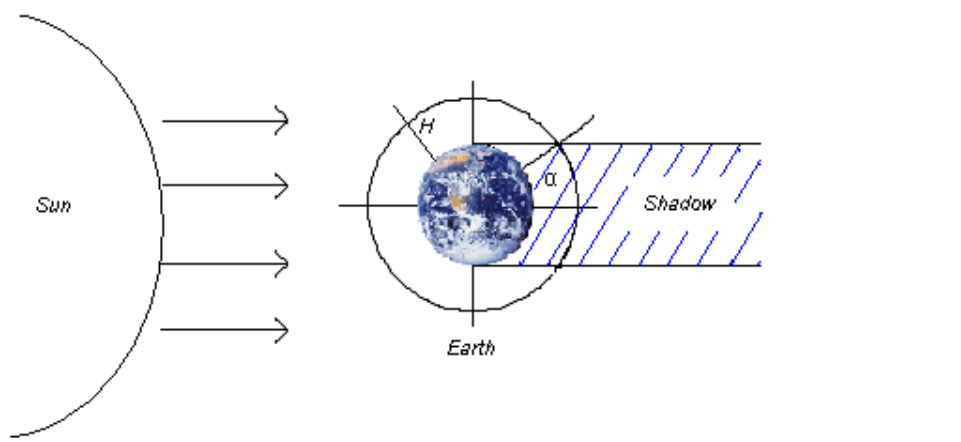

Figure 1-7 Cylindrical shadow

If the β angle is 90° the Sun vector is perpendicular to the orbital plane (*Figure 1-8*). Here the eclipse time is close to zero and the equilibrium temperature is the worst hot case temperature.

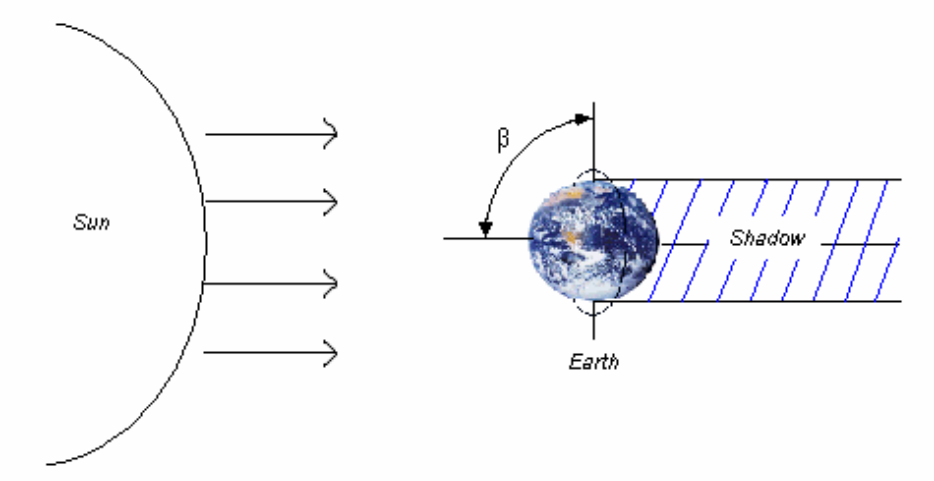

Figure 1-8 Shadow for near Sun synchronous orbit

1.2.1 Orbital revolution of Compass-1

The duration of the eclipse is important for the spacecraft's thermal design. The thermal loads from Sun and Albedo are governed by the eclipse period and influence the design of the thermal control system [R2]. Firstly, the orbit duration will be calculated:

$$t_u = \sqrt{\frac{4\pi^2}{\gamma \cdot M_E} \cdot a^3} = 96.30\,\text{min} \tag{6}$$

The approximate eclipse duration of a satellite in a circular orbit that passes the Earth's shadow represented by a circular cylinder (β=0°) can be calculated with:

$$\frac{t_E}{t_u} = \frac{2 \cdot \alpha}{360°} \tag{7}$$

where

$$\alpha = \arcsin\left(\frac{\sqrt{\left(\frac{R_E}{R}\right)^2 - \sin^2 \beta}}{\cos \beta} \right) \tag{8}$$

with

a = R = for a circular orbit = $R_E + H_a$

M_E = Mass of Earth $= 5.97 \cdot 10^{24}\,kg$

$H_a = H_p = 600km$, circular

For a 600km orbit with $\beta=0$ Compass-1 completes one orbital revolution t_u in 96.30 minutes. For two-thirds of the orbital period, t_E=60.52min, the satellite is in sunshine and its surfaces gets hot, while for 35.38 minutes it is in the Earth's shadow and cools down. Depending on this continuously changing environment a very specific and carefully designed Thermal Control System is required.

1.2.2 Earth geometry viewed from space

As mentioned the Earth emits radiation with value of around $237 \pm 21 W/m^2$. This radiation Compass-1 will receive during its orbit, in the Sun phase and the eclipse. But the value for the infrared flux depends on the distance from Earth. It decreases with the power $\dot{Q}_{IR}$:

$$\dot{Q}_{IR} = I_E A_E = I_{E(R)} A_R \tag{9}$$

where

$R = R_E + H$

A_E = surface of Earth $= 4\pi R_E^2$

A_R = radius of the sphere $= 4\pi R^2$

$I_{E(R)}$ = Earth IR depend on distance

Replacing A and R in equation (9), a new equation (10) can be written as:

$$I_{E(R)} = I_E \cdot \left(\frac{R_E^2}{(H+R)^2} \right) = I_E \cdot \sin^2 \rho' \tag{10}$$

The coverage area of a satellite is given in *Figure 1-9.*

where

$$\sin \rho' = \frac{R_E}{R_E + H}$$

ρ' =angular radius of the Earth

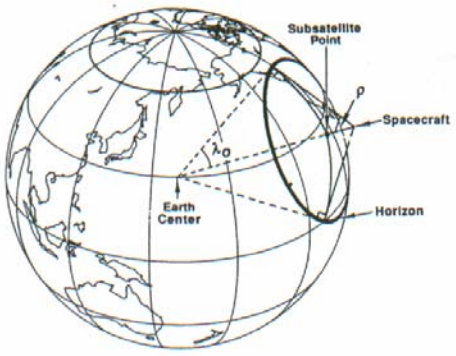

Figure 1-9 Relationship between geometry as viewed from the spacecraft and from the center of Earth (Source [R3,5])

1.3. Heat transfer

There are three fundamental thermal energy transfer mechanisms:

1. Convection
2. Conduction
3. Radiation

For each of the three transfer mechanisms, thermal energy flow is always directed from regions of higher to lower temperature. This concept is based on the Zeroth Law of Thermodynamics (thermodynamic equilibrium). It means that when two systems are put in contact with each other, energy will be exchanged between them unless they are in thermodynamic equilibrium.

1.3.1 Convection

Due to the extremely low density of the atmosphere at the orbital altitude and because of the microgravity environment, there are no mass or particles for convection processes. The surrounding background temperature in space is 3 K, very close to absolute zero. Then there is no energy transfer between hot and cold areas due to convection.

1.3.2 Conduction

When a temperature gradient is present within a continuum (gas or rigid mass), thermal energy will flow from the region of high temperature to the region of low temperature. This is known as conductive heat transfer, and is described by Fourier's Law [R12]:

$$\dot{Q}_{cond} = \frac{\lambda \cdot A \cdot \Delta T}{L} \tag{11}$$

Replacing the expression of $\dot{Q}_{cond}$ the geometrical and material properties values by a resistance factor $R_{th,cond}$, this yields to:

$$R_{th,cond} = \frac{L}{\lambda \cdot A}\left[\frac{K}{W}\right] \tag{12}$$

equation (11) can be written as:

$$\dot{Q}_{cond} = \frac{1}{R_{th.cond}} \cdot \Delta T \tag{13}$$

where

L = Length of the conduction path [m]
λ = thermal conductivity coefficient

Conduction will apply only for components on the same board and R_{jc} (thermal resistance in the junction case) can be assumed as a thermal resistance for this transfer [R12].

1.3.3 Radiation

Radiation is the only mechanism of heat transfer for which no medium is required in order to transport heat between two elements. Energy is transferred from one body to another in the form of electromagnetic radiation. Matter with a non-zero temperature emits a certain amount of radiation. The radiation energy an object emits is governed by its geometry, surface properties, relative position with respect to other thermally significant objects and its surface temperature.

$$\dot{Q}_{rad} = \varepsilon \cdot \sigma \cdot F_{ij} \cdot A \cdot T^4 \tag{14}$$

Kirchhoff's law

Kirchhoff's law states that absorptivity at any given wavelength and temperature is equal to emissivity at the same wavelength.

$$\varepsilon(\lambda, T) = \alpha(\lambda, T)$$

In general, good emitters of radiation are also good absorbers of radiation, which has to be true for the object to stay at the same temperature.

Radiation incident upon a surface can be absorbed, reflected and transmitted. Due to the conservation of this “incident radiation” the sum

$$q_i = q_\alpha + q_r + q_\tau \tag{15}$$

has to be equal to the incident radiation q_i.

Since most solid bodies used on Compass-1 are opaque to thermal radiation, transmission can be neglected.

$$q_i = q_\alpha + q_r \tag{16}$$

Planck’s law

Planck’s law gives the hemispheric intensity radiated by a black body as a function of wavelength (or frequency):

$$E_{b\lambda} = \frac{2\pi hc^2}{\lambda^5} \cdot \frac{1}{e^{ch/k\lambda T} - 1} \left[\frac{W}{m^3}\right] \tag{17}$$

where

h = Planck’s constant $6.6261 \cdot 10^{-34} Ws^2$
c = speed of light
k = Boltzmann constant

Stefan-Boltzman Law

The integration of equation (17) over all wavelengths results in the Stefan-Boltzmann-equation (18) which represents the total of amount of radiated energy for a black body.

$$\int dE_{b\lambda} = \int \frac{2\pi hc^2}{\lambda^5} \cdot \frac{1}{e^{ch/k\lambda T} - 1} d\lambda = \left[\frac{W}{m^2}\right]$$

$$\sigma = \frac{2\pi^5 k^4}{15c^2}$$

Stefan-Boltzmann law :

$$I = \sigma T^4 \left[\frac{W}{m^2} \right] \tag{18}$$

Wien's displacement law

The wavelength $\lambda_{\max}$, for which the radiated power per unit of wavelength is maximal, is related to the temperature T of the thermal emitter.

$$\lambda_{\max} T = const. = C_3 \tag{19}$$

$C_3 =$ constant in Wien's displacement law $0.28978 \left[\frac{cm}{K} \right]$

Thus the hotter an object the lower is the wavelength for the maximum radiation intensity. An object that glows bluish is hotter and brighter then an object that glows red (the wavelength of blue light is shorter than that of red light).

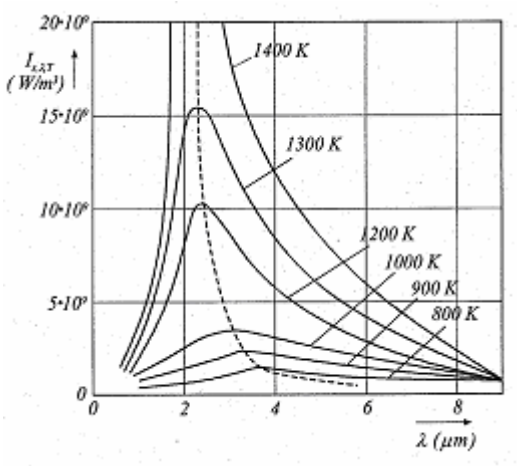

Figure 1-10 Wien's displacement law

2. Calculations

In this chapter preliminary thermal calculations will be done in order to have an idea of the temperature Compass-1 will have to withstand during its life time. Several cases with various coatings are considered to choose surface properties for Compass-1, operating in acceptable temperature limits.

2.1. Energy balance of Compass-1

Thermal heat balance for steady-state happens when the amount of heat coming into the spacecraft equals the amount of heat leaving the spacecraft. Heat from the space environment is largely the result of solar radiation. Heat is lost from the spacecraft by radiation, mainly to deep space. In Addition the influence of Earth is included. [R13]

$$\dot{Q}_{in} = \dot{Q}_{out} \tag{20}$$

$$\dot{Q}_{sun} + \dot{Q}_{albedo} + \dot{Q}_{earth} + \dot{Q}_{P} = \dot{Q}_{sat \to earth} + \dot{Q}_{sat \to space} \tag{21}$$

where

$$\dot{Q}_{sun} = \alpha_s A_{sat,proj} I_{sun}$$
$$\dot{Q}_{albedo} = \alpha_s A_{sat} F_{earth \to sat} 0.34 \cdot I_{sun}$$
$$\dot{Q}_{earth} = \alpha_{IR} A_{sat} F_{earth \to sat} I_{earth}$$
$$\dot{Q}_{sat \to earth} = \varepsilon_{IR} A_{sat} F_{sat \to earth} \sigma (T_{sat}^4 - T_{earth}^4)$$
$$\dot{Q}_{sat \to space} = \varepsilon_{IR} A_{sat} F_{sat \to space} \sigma (T^4 - T_{space}^4)$$

$$A_{sat} F_{earth \to sat} = A_p$$
$$A_{sat} F_{space \to sat} = 6 \cdot A_p - \left(A_{sat} F_{earth \to sat}\right) = 5 \cdot A_p$$
$$A_{sat} F_{sat \to earth} = A_p$$
$$A_{sat} F_{sat \to space} = 6 \cdot A_p - \left(A_{sat} F_{sat \to earth}\right) = 5 \cdot A_p$$

$\alpha_{IR} = \varepsilon_{IR}$ (for temperature radiation)
$\dot{Q}_P$ = electrical power dissipation

2.2. Properties of materials

Surface

The external surfaces of a spacecraft radiatively couple the spacecraft to space. Because these surfaces are also exposed to external sources of energy such as solar radiation, Albedo and Earth-emitted IR, their radiative properties must be selected to achieve an energy balance at the desired temperature limits.
For Compass-1 the used materials with their properties are shown in the following *Table2-1*.

	Al 6061-T6	Solar cells	Black paint
Density [kg/m^3]	2700	2100	-
Conductivity [W/(m*K)]	166.9	200	-
Specific Heat [J/(kg*K)]	980	1600	-
Emissivity (thermal)	0.08	0.85	0.90
Absorptivity (solar)	0.379	0.92	0.97

Table 2-1 Material properties of Compass-1

Satellite structure

The basis structure is made from Al 6061-T6 [R11]. The optical surface properties are shown in *Table 2-1*, they are based on an uncoated surfaces.

Solar cells

Due to their high absorptivity, high emissivity, and low thermal mass, solar arrays typically cycle over wide temperature ranges as they go from sunlight to eclipse. The most advanced one are from RWE/Germany with an efficiency of 28.0%. They are Ultra Triple Junction Solar Cells [R10].

Black paint

The paint Nextel, Velvet-Coating 2010, 3M Comp. has been certified for space conditions like vacuum and extreme temperature ranges. This paint will be considered for a surface finish, because of the high absorptivity. This may be interesting in the shadow phase [R9].

The surface of Compass-1 is made up of about 30% aluminum alloy and 70% solar cells. Hence, it is necessary to calculate an average material property for the thermal analysis with

$$\dot{Q}_{A_p} = \dot{Q}_{sc} + \dot{Q}_{Al} \tag{22}$$

where

$$\dot{Q}_{sc} = \varepsilon_{sc} \cdot A_{sc} \cdot \sigma \cdot T_{sc}^4$$
$$\dot{Q}_{Al} = \varepsilon_{Al} \cdot A_{Al} \cdot \sigma \cdot T_{Al}^4$$
$$T_{Al} = T_{sc}$$

using the equation (22)

$$\varepsilon_{Al-Sc} \cdot A_p \cdot \sigma \cdot T^4 = \sigma \cdot T^4 \left(\varepsilon_{sc} \cdot A_{sc} + \varepsilon_{Al} \cdot A_{Al}\right)$$
$$\varepsilon_{Al-Sc} = \varepsilon_{sc} \cdot \frac{A_{sc}}{A_p} + \varepsilon_{Al} \cdot \frac{A_{Al}}{A_p}$$

For the sides 1,2,3,6 (covered with 70% solar cells and 30% aluminum) it follows:

$$\alpha_{Al-Sc} = 0.7 \cdot 0.92 + 0.3 \cdot 0.379 = 0.76$$
$$\varepsilon_{Al-Sc} = 0.7 \cdot 0.85 + 0.3 \cdot 0.08 = 0.62$$

For the side 5, which aluminum parts are black painted and, the average value is:

$$\alpha_{Bp-Sc} = 0.7 \cdot 0.92 + 0.3 \cdot 0.97 = 0.94$$
$$\varepsilon_{Bp-Sc} = 0.7 \cdot 0.85 + 0.3 \cdot 0.9 = 0.865$$

Solar cells will not be attached to side 4, because of antenna design. On this side the communication antenna and GPS antenna will be mounted and on this side no solar cells will be attached because of the size of the solar cells.

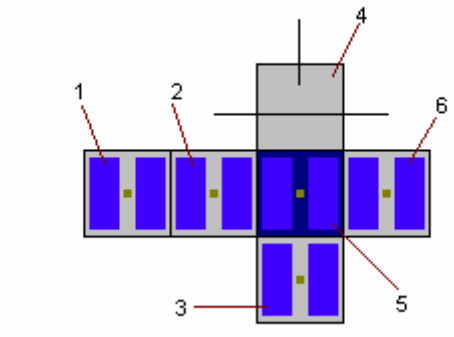

Figure 2-1 Structure of Compass-1

Cube surface	ε	α	Coverage
1	0.62	0.76	70% Sc, 30% Al
2	0.62	0.76	70% Sc, 30% Al
3	0.62	0.76	70% Sc, 30% Al
4	0.08	0.379	100% Al
5	0.865	0.94	70% Sc, 30% Bp
6	0.62	0.76	70% Sc, 30% Al

Table 2-2 Average of optical surface properties for partial covered surfaces

Further calculations follows the plan shown in *Figure* 2-2 .

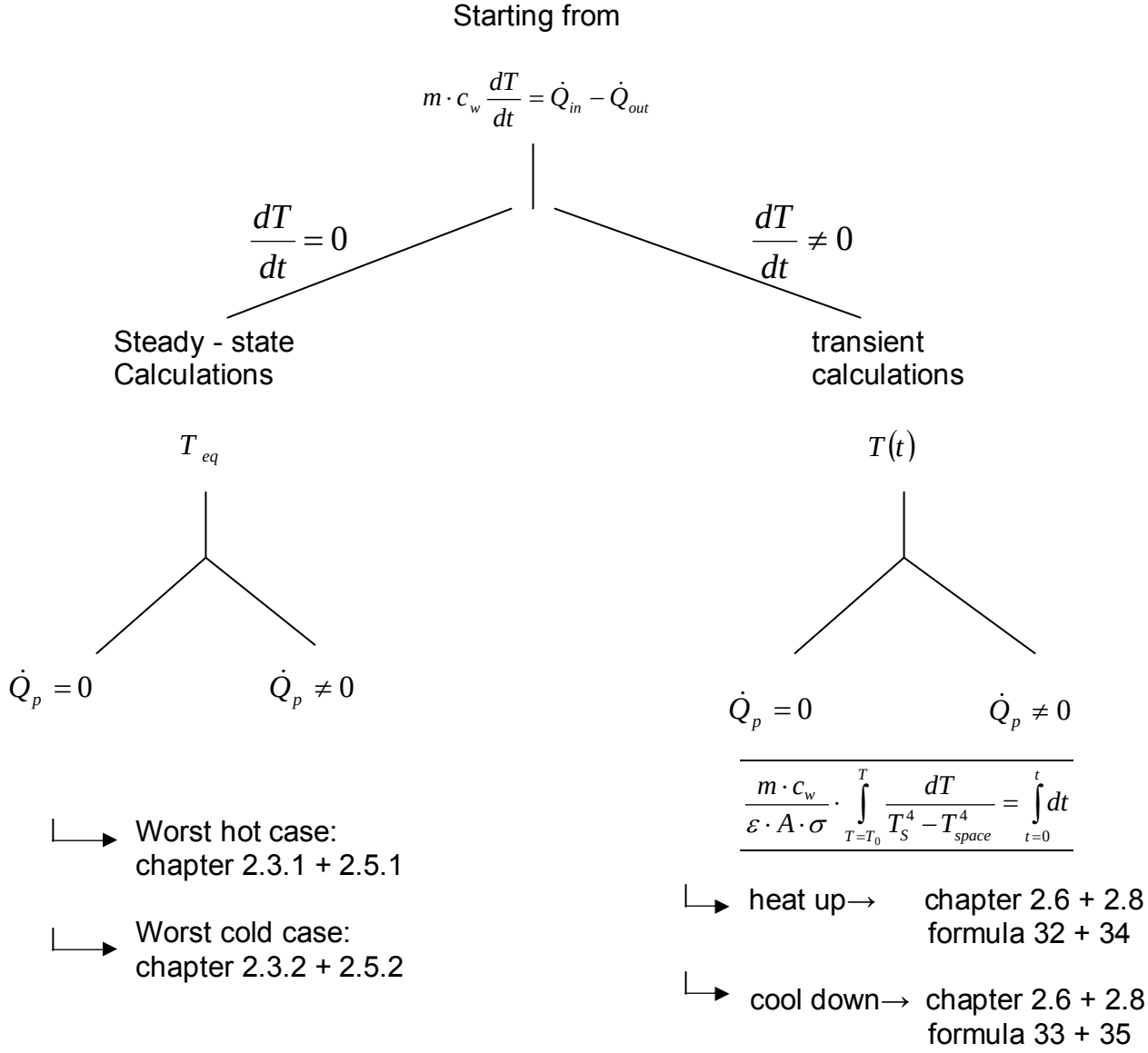

Figure 2-2 Approach to the calculations

2.3 Temperature equilibrium

This section presents calculations of steady-state equilibrium temperatures on Compass-1. As already mentioned the calculations are used as a means of first order approximation of the expected temperatures on orbit for Compass-1. Two main cases are considered: worst hot case and worst cold case. The general dependence of local equilibrium temperature in Compass-1 included emissivity, solar absorptivity, solar radiation, Albedo, Earth radiation and radiation from body to space. The objective is the computation of the equilibrium temperature for Compass-1, considering no internal heat sources at this stage, such that

$$\dot{Q}_p = 0$$

Radiation balance

The calculation of the steady-state temperatures uses a basic energy balance. The equilibrium temperature is obtained from condition $\dot{Q}_{in} = \dot{Q}_{out}$ (see chapter 2.1, equation (22)). The effects included in the calculation are solar radiation, Albedo, Earth radiation and radiation from the body to space.

$$\boxed{\varepsilon^*_{IR}\sigma \cdot 5A_p\left(T^4 - T^4_{space}\right) + \varepsilon_{IR}\sigma A_p\left(T^4 - T^4_E\right) = \alpha_{S_S} I_S A_p + 0.34\,\alpha_{S_B} I_S A_p + \alpha_{IR} I_E A_p} \quad (23)$$

The part $\varepsilon_{IR}\sigma A_p\left(T^4 - T_E^4\right)$ can be neglected, because $T_E \approx T$.
Therefore it is assumed that $\left(T^4 - T_E^4\right) \cong 0$

The equation after solving for equilibrium temperature (worst hot case) is:

$$\boxed{T = \sqrt[4]{\frac{\alpha_{S_2}}{\varepsilon^*_{IR}} \cdot \frac{I_s}{\sigma} \cdot \frac{A_p}{5A_p} + \frac{\alpha_{S_1}}{\varepsilon^*_{IR}} \cdot \frac{0.34 I_s}{\sigma} \cdot \frac{A_p}{5A_p} + \frac{\alpha_{IR}}{\varepsilon^*_{IR}} \cdot \frac{A_p}{5A_p} \cdot \frac{I_E}{\sigma} + T^4_{space}}} \quad (24)$$

In the following sections different possibilities of the surface finish of Compass-1 are examined. There are several feasible options for surface finish, so the purpose of this chapter is to choose a suitable solution for Compass-1 on its orbit.

2.3.1 Worst hot case

For a solar array covered body of a spacecraft, the energy balance equation includes a power generation term since the solar cells convert solar energy directly to electrical energy. Therefore there is 1W dissipation inside the cube.

The worst hot case temperature for Compass-1 with non operating solar cells is given by:

$$T_{\max} = \left[T_{space}^4 + \underbrace{\frac{I_s}{\sigma} \cdot \frac{A_p}{5A_p} \cdot \frac{\alpha_{S_S}}{\varepsilon_{IR}^*}}_{Sun} + \underbrace{\frac{I_E}{\sigma} \cdot \frac{A_p}{5A_p} \cdot \frac{\varepsilon_{IR}}{\varepsilon_{IR}^*}}_{IR} + \underbrace{\frac{0.34 \cdot I_s}{\sigma} \cdot \frac{A_p}{5A_p} \cdot \frac{\alpha_{S_B}}{\varepsilon_{IR}^*}}_{Albedo} \right]^{1/4} \quad (25)$$

where

α_{S_S} = solar Absorptivity

α_{S_B} = solar Absorptivity of bottom

ε_{IR}^* = average emissivity value, for the sum of the areas, which interacts with deep space

$\alpha_{IR} = \varepsilon_{IR}$ using the Kirchhoff´s law

Results for various surface properties for worst hot case:

Solar radiated surface covered with 70% solar cells and 30% aluminum

Orientated side to Earth	
70% solar cells and 30% aluminum	70% solar cells and 30% black paint
$\varepsilon_{IR_1} = 0.62^{1)}, \alpha_{S_S} = 0.76^{1)}$ $\varepsilon_{IR}^* = 0.512^{2)}, \alpha_{S_B} = 0.76^{1)}$	$\varepsilon_{IR_1} = 0.865^{1)}, \alpha_{S_S} = 0.76^{1)}$ $\varepsilon_{IR}^* = 0.512^{2)}, \alpha_{S_B} = 0.94^{1)}$
$T_{\max} = 320.8K$	$T_{\max} = 325.1K$

Solar radiated surface covered with 100% aluminum

Orientated side to Earth	
70% solar cells and 30% aluminum	70% solar cells and 30% black paint
$\varepsilon_{IR_1} = 0.62^{1)}, \alpha_{S_S} = 0.379$ $\varepsilon^*_{IR} = 0.512^{2)}, \alpha_{S_B} = 0.76^{1)}$	$\varepsilon_{IR_1} = 0.865^{1)}, \alpha_{S_S} = 0.379$ $\varepsilon^*_{IR} = 0.512^{2)}, \alpha_{S_B} = 0.94^{1)}$
$T_{\max} = 289.2K$	$T_{\max} = 295.0K$

Solar radiated surface coverage with 70% solar cells and 30% black paint

Orientated side to Earth	
70% solar cells and 30% aluminum	70% solar cells and 30% black paint
$\varepsilon_{IR_1} = 0.62^{1)}, \alpha_{S_S} = 0.94^{1)}$ $\varepsilon^*_{IR} = 0.886^{3)}, \alpha_{S_B} = 0.76^{1)}$	$\varepsilon_{IR_1} = 0.865^{1)}, \alpha_{S_S} = 0.94^{1)}$ $\varepsilon^*_{IR} = 0.886^{3)}, \alpha_{S_B} = 0.94^{1)}$
$T_{\max} = 290.3K$	$T_{\max} = 287.9K$

Solar radiated surface covered with 100% black paint

Orientated side to Earth	
70% solar cells and 30% aluminum	70% solar cells and 30% black paint
$\varepsilon_{IR_1} = 0.62^{1)}, \alpha_{S_S} = 0.97$ $\varepsilon^*_{IR} = 0.886^{3)}, \alpha_{S_B} = 0.76^{1)}$	$\varepsilon_{IR_1} = 0.865^{1)}, \alpha_{S_S} = 0.97$ $\varepsilon^*_{IR} = 0.886^{3)}, \alpha_{S_B} = 0.94^{1)}$
$T_{\max} = 286.1K$	$T_{\max} = 289.6K$

2.3.2 Worst cold case eclipse

If the spacecraft is in the shadow of the Earth and is not in view of any portion of the Sun's radiation, this condition is called a worst cold case condition. For this condition there is no direct solar, albedo energy intake, which also means, that no electric power can be generated by the solar cells. In this case the equation for the equilibrium temperature is reduced to equation (26):

$$T_{\min} = \left[T_{space}^4 + \frac{I_E}{\sigma} \cdot \frac{\varepsilon_{IR}}{\varepsilon_{IR}^*} \cdot \frac{A_p}{5A_p} \right]^{1/4} \tag{26}$$

This cases are distinguished by two possibilities of coverage of the satellites bottom. In first case the bottom consists of 70% solar cells and 30% aluminum, in the second case 70% solar cells and 30% black paint. Using the Kirchhoff's law $\alpha_{IR} = \varepsilon_{IR}$:

where

ε_{IR} = IR emissivity value

ε_{IR}^* = average emissivity value, for the sum of the areas, which interacts with to deep space

Results for various surface properties for worst cold case:

Results for covered side with 70% solar cells and 30% aluminum

Orientated side to Earth	
70% solar cells and 30% aluminum	70% solar cells and 30% black paint
$\varepsilon_{IR} = 0.62^{1)}$ $\varepsilon_{IR}^* = 0.512^{2)}$	$\varepsilon_{IR} = 0.865^{1)}$ $\varepsilon_{IR}^* = 0.512^{2)}$
$T_{\min} = 177.0K$	$T_{\min} = 192.4K$

Results for covered side with 70% solar cells and 30% black paint

Orientated side to Earth	
70% solar cells and 30% aluminum	70% solar cells and 30% black paint
$\varepsilon_{IR} = 0.62$[1)] $\varepsilon_{IR}^{*} = 0.886$[3)]	$\varepsilon_{IR} = 0.865$[1)] $\varepsilon_{IR}^{*} = 0.886$[3)]
$T_{\min} = 154.4K$	$T_{\min} = 167.7K$

[1)] The values are calculated in chapter 2.4

[2)] The areas which radiates into deep space are 4 sides covered with 70% solar cells and 30% aluminum and one side with 100% aluminum.

$$\varepsilon_{IR}^{*} = \frac{4 \cdot \varepsilon_{Sc-Al} + 1 \cdot \varepsilon_{Al}}{5} = \frac{4 \cdot 0.62 + 0.08}{5} = 0.512$$

[3)] The areas which radiates into deep space are 4 sides covered with 70% solar cells and 30% black paint and one side with 100% black paint.

$$\varepsilon_{IR}^{*} = \frac{4 \cdot \varepsilon_{Sc-Bp} + 1 \cdot \varepsilon_{Bpl}}{5} = \frac{4 \cdot 0.865 + 0.97}{5} = 0.886$$

2.3. Summary for stationary calculations

		Stationary calculations	
Coverage (Sun radiated side)	Values	bottom 70% solar cells 30% aluminum	bottom 70% solar cells 30% black paint
70% solar cells 30% aluminum	T_{max}	320.8K	325.1K
	T_{min}	177.0K	192.4K
100% aluminum	T_{max}	289.2K	295.0K
	T_{min}	177.0K	192.4K
70% solar cells 30% black paint	T_{max}	290.3K	287.9K
	T_{min}	154.4K	167.7K
100% black paint	T_{max}	286.1K	289.6K
	T_{min}	154.4K	167.7K

Table 2-3 Results of steady-state calculations

- The results from the hot case calculations yield the following conclusions:

  The temperature values are different from each other for various coatings. With the temperature values for the Sun radiated side covered with 70% solar cells 30% aluminum the overall temperature of the battery (*Table1-1*) is about 30°C above its maximum hot operational limit. With the other surface properties the battery is able to survive during the Sun phase.

- The cold case predictions yield worse conditions. The temperature of every satellite subsystem will dip below the cold limits for eclipse equilibrium temperature. With the temperature values between T_{min} =192.4 K and T_{min} =154.4 K the satellite is too cold.

2.4. Temperature equilibrium with electrical power dissipation on board

In this chapter the calculations for the equilibrium temperature include the dissipated power, which is present inside the satellite. The computation ensues from chapter 2.2, whereby the following formula (27) with $Q_p = 1W$ will be applied:

$$\boxed{\varepsilon_{IR}^{*}\sigma \cdot 5A_p\left(T^4 - T_{space}^4\right) + \varepsilon_{IR}\sigma A_p\left(T^4 - T_E^4\right) = \alpha_{S_S} I_S A_p + 0.34\,\alpha_{S_B} I_S A_p + \alpha_{IR} I_E A_p + \dot{Q}_p} \qquad (27)$$

using the Kirchhoff´s law $\alpha_{IR} = \varepsilon_{IR}$

2.5.1 Worst hot case with electrical power dissipation

Using equation (25) the worst hot case with electrical power dissipation $\dot{Q}_p = 1W$ can be calculated with:

$$T_{\max} = \left[T_{space}^4 + \frac{I_s}{\sigma} \cdot \frac{A_p}{5A_p} \cdot \frac{\alpha_{S_S}}{\varepsilon_{IR}^{*}} + \frac{I_E}{\sigma} \cdot \frac{A_p}{5A_p} \cdot \frac{\varepsilon_{IR}}{\varepsilon_{IR}^{*}} + \frac{0.34 \cdot I_s}{\sigma} \cdot \frac{A_p}{5A_p} \cdot \frac{\alpha_{S_B}}{\varepsilon_{IR}^{*}} + \frac{\dot{Q}_p}{\varepsilon_{IR}^{*} 5A_p \sigma} \right]^{1/4} \qquad (28)$$

where

α_{S_S}	= solar Absorptivity
α_{S_B}	= solar Absorptivity of bottom
ε_{IR}	= IR emissivity value
ε_{IR}^{*}	= average emissivity value, for the sum of the areas, which interacts with deep space

Calculations:

Solar radiated surface covered with 70% solar cells and 30% aluminum

Orientated side to Earth	
70% solar cells and 30% aluminum	70% solar cells and 30% black paint
$\varepsilon_{IR_1} = 0.62^{1)}, \alpha_{S_S} = 0.76^{1)}$ $\varepsilon^*_{IR} = 0.512^{2)}, \alpha_{S_B} = 0.76^{1)}$	$\varepsilon_{IR_1} = 0.865^{1)}, \alpha_{S_S} = 0.76^{1)}$ $\varepsilon^*_{IR} = 0.512^{2)}, \alpha_{S_B} = 0.94^{1)}$
$T_{\max} = 326.0K$	$T_{\max} = 330.0K$

Solar radiated surface covered with 100% aluminum

Orientated side to Earth	
70% solar cells and 30% aluminum	70% solar cells and 30% black paint
$\varepsilon_{IR_1} = 0.62^{1)}, \alpha_{S_S} = 0.379$ $\varepsilon^*_{IR} = 0.512^{2)}, \alpha_{S_B} = 0.76^{1)}$	$\varepsilon_{IR_1} = 0.865^{1)}, \alpha_{S_S} = 0.379$ $\varepsilon^*_{IR} = 0.512^{2)}, \alpha_{S_B} = 0.94^{1)}$
$T_{\max} = 296.1K$	$T_{\max} = 305.0K$

Solar radiated surface covered with 70% solar cells and 30% black paint

Orientated side to Earth	
70% solar cells and 30% aluminum	70% solar cells and 30% black paint
$\varepsilon_{IR_1} = 0.62^{1)}, \alpha_{S_S} = 0.94^{1)}$ $\varepsilon^*_{IR} = 0.886^{3)}, \alpha_{S_B} = 0.76^{1)}$	$\varepsilon_{IR_1} = 0.865^{1)}, \alpha_{S_S} = 0.94^{1)}$ $\varepsilon^*_{IR} = 0.886^{3)}, \alpha_{S_B} = 0.94^{1)}$
$T_{\max} = 294.3K$	$T_{\max} = 299.6K$

Solar radiated surface covered with 100% black paint

Orientated side to Earth	
70% solar cells and 30% aluminum	70% solar cells and 30% black paint
$\varepsilon_{IR_1} = 0.62^{1)}, \alpha_{S_S} = 0.97$ $\varepsilon^*_{IR} = 0.886^{3)}, \alpha_{S_B} = 0.76^{1)}$	$\varepsilon_{IR_1} = 0.865^{1)}, \alpha_{S_S} = 0.97$ $\varepsilon^*_{IR} = 0.886^{3)}, \alpha_{S_B} = 0.94^{1)}$
$T_{\max} = 295.9K$	$T_{\max} = 301.1K$

2.5.2 Worst cold case with electrical power dissipation

In this case only four cases need to be examined, because the Earth orientated surface consists of 70% solar cells/30% aluminum either 70% solar cells/30% black paint. However, the different ε^*_{IR} has to be considered. The average ε^*_{IR} and ε_{IR} are calculated in chapter 2.3.1 and 2.3.2.

$$T_{\min} = \left[T^4_{space} + \frac{I_E}{\sigma} \cdot \frac{\varepsilon_{IR}}{\varepsilon^*_{IR}} \cdot \frac{A_p}{5A_p} + \frac{\dot{Q}_p}{\varepsilon^*_{IR} 5 A_p \sigma} \right]^{1/4} \tag{29}$$

where

ε_{IR} = IR emissivity value

ε^*_{IR} = average emissivity value, for the sum of the areas, which interacts with deep space

A_p = surface area of one side of the cube

Results for various surface properties for worst cold case:

Values for coverage with 70% solar cells and 30% aluminum, and 100% aluminum on side number 4.

Orientated side to Earth	
70% solar cells and 30% aluminum	70% solar cells and 30% black paint
$\varepsilon_{IR} = 0.62$ $\varepsilon^*_{IR} = 0.512$	$\varepsilon_{IR} = 0.865$ $\varepsilon^*_{IR} = 0.512$
$T_{\min} = 202.2K$	$T_{\min} = 213.0K$

Values for coverage with 70% solar cells and 30% black paint, and 100% black paint on side number 4.

Orientated side to Earth	
70% solar cells and 30% aluminum	70% solar cells and 30% black paint
$\varepsilon_{IR} = 0.62$ $\varepsilon^*_{IR} = 0.886$	$\varepsilon_{IR} = 0.865$ $\varepsilon^*_{IR} = 0.886$
$T_{\min} = 176.3K$	$T_{\min} = 185.7K$

Summary for steady-state calculations:

		Stationary calculations	
Coverage (illuminated side)	Values	bottom 70% solar cells 30% aluminum	bottom 70% solar cells 30% black paint
70% solar cells 30% aluminum	T_{max}	326.0K	330.0K
	T_{min}	202.2K	213.0K
100% aluminum	T_{max}	296.1K	305.0K
	T_{min}	202.2K	213.0K
70% solar cells 30% black paint	T_{max}	294.3K	299.6K
	T_{min}	176.3K	185.7K
100% black paint	T_{max}	295.9K	301.1K
	T_{min}	176.3K	185.7K

Table 2-4 Results for steady state calculations with electrical power dissipation

- The results of the worst cold case including heat dissipation shows, that the dissipation is not able to increase the temperature inside Compass-1 during the eclipse so that the components are within the allowable temperature limits.
  Compared with the temperature values for worst cold case from chapter 2.4 the values in this case rose around 20°, but this is not sufficient for the satellite overall temperature behavior, especially for the battery and camera operation temperature limits.

- The results from the worst hot case calculation yield that the temperatures for the Sun radiated side covered with 70% solar cells and 30% aluminum is too high for battery and camera.
  For the Sun radiated side covered by 70% solar cells and 30% black paint the temperature is within the allowable limits, but the temperatures determined on Compass-1 are very low.

- Due to this low temperature values, probably a heater will be needed, which will keep the satellite and its interior components in their required operating temperature ranges during the shadow phase.

2.5. Instationary calculation

This section shows a detailed calculation of instationary conditions for coverage with 70% solar cells and 30% aluminum, and black painted bottom. The calculations for the further cases are attached in Appendix B.

Using the equations (25) in chapter 2.3.1 and (26) in chapter 2.3.2 the equilibrium temperatures are:

* For the cold case at the end of eclipse: $T_{\min} = 192.4K$
* For the hot case in Sun: $T_{\max} = 325.1K$

Instationary calculation [1]:

The temperature extremes for Compass-1 as a one mass thermal node have been calculated in the previous sections. The analytical means discussed in these sections allows the computation of the temperature varying with time between the two steady-state boundary conditions. In order to be able to calculate the transient thermal behavior of Compass-1, a basic instationary equation has to be considered:

$$m \cdot c_w \cdot \frac{dT}{dt} = \dot{Q}_{in} - \dot{Q}_{out} \tag{30}$$

This equation can be solved in a first step for the equilibrium condition $\frac{dT}{dt} = 0$,

$$\dot{Q}_{in} = \dot{Q}_{out}$$

Using the general formulation of the equilibrium calculation (T_{max}, T_{min}) for solving the instationary basic equation a nonlinear differential equation emerges, which can be easily solved by separating the variables and subsequent integration.

In case of no internal energy dissipation, the separated differential equation is [1]:

$$\frac{m \cdot c_w}{\varepsilon \cdot A \cdot \sigma} \cdot \int_{T=T_0}^{T} \frac{dT}{T_S^4 - T_{space}^4} = \int_{t=0}^{t} dt \tag{31}$$

Integrating this equation for the heating up phase $(T_a > T_0)$ results:

$$\Delta t_{heat} = c \cdot \left[\left(ar\tanh\left(\frac{T_a}{T_S}\right) + \arctan\left(\frac{T_a}{T_S}\right)\right) - \left(ar\tanh\left(\frac{T_0}{T_S}\right) + \arctan\left(\frac{T_0}{T_S}\right)\right)\right] \qquad (32)$$

where (calculation for solar radiated coverage with 70% solar cells and 30% aluminum and black painted bottom)

$T_S = T_{\max}$ = 325.1K
$T_o =$ starting temperature of calculation = 192.4K
$T_a =$ actual temperature

In case of down cooling the satellite the integration results in

$$\Delta t_{cool} = c \cdot \left[\left(ar\coth\left(\frac{T_a}{T_E}\right) + \arctan\left(\frac{T_a}{T_E}\right)\right) - \left(ar\coth\left(\frac{T_0}{T_E}\right) + \arctan\left(\frac{T_0}{T_E}\right)\right)\right] \qquad (33)$$

where

$T_E = T_{\min}$ = 192.4K
$T_o =$ starting temperature of calculation = $T_{a_{sun1}} > T_a$
$T_a =$ actual temperature

The constant “c” for the satellite is given by:

<u>for the heating up phase</u>

$$c_S = \frac{\frac{\sum m_i \cdot c_{w_i}}{\varepsilon_A \cdot A \cdot \sigma}}{2 \cdot T_S^3} = 2310s$$

<u>for the cooling down phase</u>

$$c_E = \frac{\frac{\sum m_i \cdot c_{w_i}}{\varepsilon_A \cdot A \cdot \sigma}}{2 \cdot T_E^3} = 11143s$$

where

T_S = 325.1K , T_E = 192.4K

m_{Al} = 270g and $c_{w_{Al}} = 980\frac{Nm}{kg \cdot K}$

m_{SC} = 27g and $c_{w_{SC}} = 1600\frac{Nm}{kg \cdot K}$

ε_A = average emissivity value for the satellite

$$\begin{aligned}
\dot{Q}_A &= 4 \cdot \dot{Q}_{Al-Sc} + 1 \cdot \dot{Q}_{Bp-Sc} + 1 \cdot \dot{Q}_{Al} \\
\varepsilon_A \sigma T^4 A_T &= \sigma T^4 (4A \cdot \varepsilon_{Al-Sc} + 1A \cdot \varepsilon_{Bp-Sc} + 1A \cdot \varepsilon_{Al}) \\
\varepsilon_A &= \frac{4}{6} \cdot \varepsilon_{Al-Sc} + \frac{1}{6} \cdot \varepsilon_{Bp-Sc} + \frac{1}{6} \cdot \varepsilon_{Al} = 0.57
\end{aligned}$$

2.6. Results of instationary calculation

Starting with the equilibrium temperatures in hot and cold phase, the temperature behavior during the circulation on orbit can now step by step be calculated.

If the starting point is assumed at the end of the shadow phase and uses the calculated (chapter 1.2.1) time span of the Sun phase of 60.52min, the temperature just before entering the shadow is

$$\Delta t_{sun} = 60.52\,\text{min} \quad \rightarrow \quad \begin{matrix} T_0 = T_{\min} \\ T_{sun1} \end{matrix}$$

This is the start temperature for the cooling phase calculation in the Earth's shadow (30.38min).

$$\Delta t_E = 35.38\,\text{min} \quad \rightarrow \quad \begin{matrix} T_0 = T_{sun1} \\ T_{E1} \end{matrix}$$

This calculation can be done several times up to a point where the Sun and shadow end temperatures do not change any more, i.e. an abort condition of ε ≤ ± 1K is reached. *Table2-5* shows the results for a period of 3 orbits, to determine which temperature values will be reached.

Instationary calculations							
Coverage (illuminated side)	Values	bottom 70% solar cells 30% aluminum			bottom 70% solar cells 30% black paint		
		1.Orbit	2.Orbit	3.Orbit	1.Orbit	2.Orbit	3.Orbit
70% solar cells 30% aluminum	T_S	302.8K	314.5K	315.0K	313.8K	320.6K	320.8K
	T_E	247.1K	251.3K	251.5K	251.6K	253.7K	253.8K
100% aluminum	T_S	264.2K	279.3K	280.8K	278.5K	288.0K	288.5K
	T_E	230.8K	237.7K	238.3K	238.9K	242.6K	242.8K
70% solar cells 30% black paint	T_S	278.7K	286.2K	286.5K	279.2K	284.4K	284.6K
	T_E	219.3K	221.7K	221.8K	220.7K	222.3K	222.4K
100% black paint	T_S	273.5K	281.7K	281.9K	281.5K	286.3K	286.4K
	T_E	217.6K	220.3K	220.3K	221.3K	222.8K	222.8K

Table 2-5 Results of the transient temperature calculation

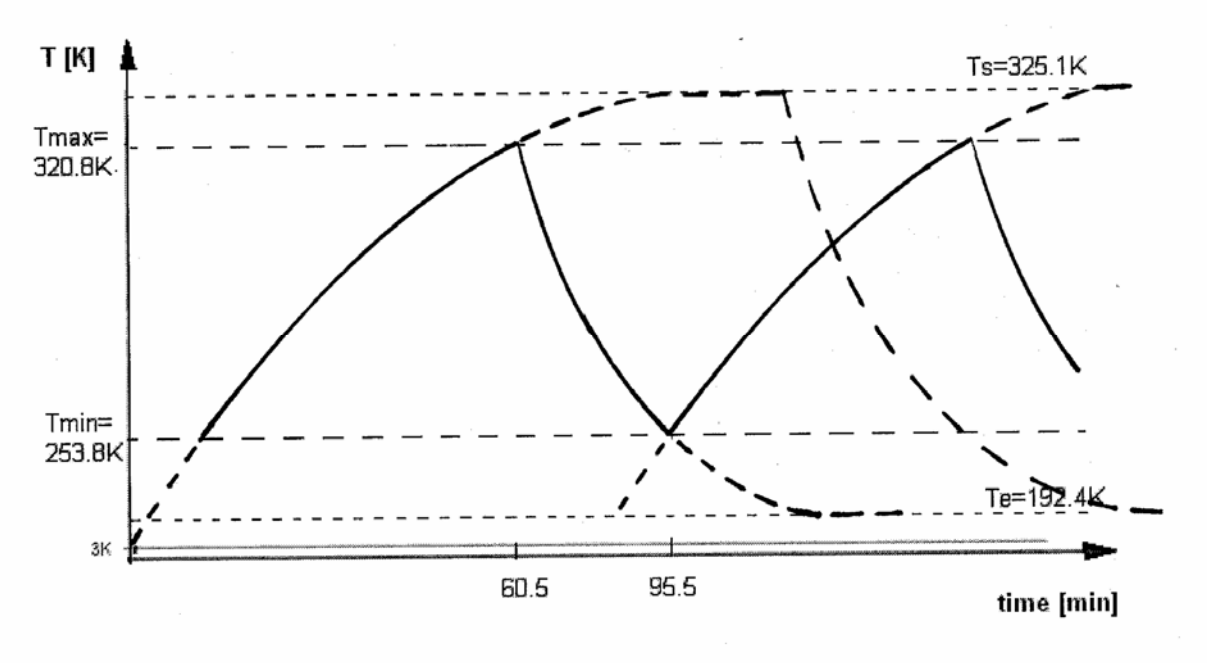

Figure 2-3 Temperature behavior during one Earth orbit
(coverage: solar radiated surface: 70% Sc and 30% Al
bottom: 70% Sc and 30% Bp)

- The first results from the instationary calculation yield that the coverage with 70% solar cells and 30% aluminum and the coverage with 70% solar cells is a possible solution to control the satellite. For the aluminum application the temperatures during the Sun period for this coverage are too hot for the battery, but in the eclipse the temperatures are most nearly to the lower temperature limit. The battery is the most thermal sensitive part of the satellite subsystems because it can not be recharged below +5°C.

- The secondary choice of surface finish which can be taken into consideration is the coverage with solar cells and black paint on each surface. The temperature values for the Sun period are within the allowable temperature limits. Only during the eclipse a temperature control has to be developed.

- Because Compass-1 rotates during his orbit along the z-axis the sides with 100% aluminum and 100% black paint can also be exposed to solar radiation. These cases were considered and computed as well.

- This first result shows also, that the temperature values with solar cells and black painted side, which is orientated to the Earth, are higher than the values with solar cells and aluminum coverage. Thus a first tendency shows for the surface finish for the Earth orientated side preferred in black resulting in a higher temperature in order of 2 degrees.

- *Figure 2-3* shows the temperature characteristics of Compass-1 during its time in orbit. After the satellite heats up in the Sun phase to T_{max} =320.8K, it enters into the shadow and the maximum equilibrium temperature T_S =325.1K cannot be reached. This same scenario occurs during the eclipse.

2.7. Instationary calculation with electrical power dissipation

Solar radiated surface is covered with 70% solar cells and 30% aluminum and the Earth orientated side is a black painted bottom with 70% solar cells.

The instationary temperature calculations can be proceeded with the boundary conditions in chapter 2.5.1 and chapter 2.5.2 (T_{max}=330K and T_{min}=213K). The calculations ensue according to the same principle as in chapter 2.6 with the equation (32) for the heating up phase with a time span Δt_{Sun}=60.52min and the equation (33) for the cooling down phase with Δt_{Shadow}=35.38min.

Equation for the heating up phase is:

$$\Delta t_{heat} = c \cdot \left[\left(ar\tanh\left(\frac{T_a}{T_S}\right) + \arctan\left(\frac{T_a}{T_S}\right)\right) - \left(ar\tanh\left(\frac{T_0}{T_S}\right) + \arctan\left(\frac{T_0}{T_S}\right)\right)\right] \qquad (34)$$

where

$T_S = T_{\max} = 330K$

$T_0 =$ starting temperature of calculation = 213.0K

$T_a =$ actual temperature

In case of cooling down the equation is:

$$\Delta t_{cool} = c \cdot \left[\left(ar\coth\left(\frac{T_a}{T_E}\right) + \arctan\left(\frac{T_a}{T_E}\right)\right) - \left(ar\coth\left(\frac{T_0}{T_E}\right) + \arctan\left(\frac{T_0}{T_E}\right)\right)\right] \qquad (35)$$

where

$T_E = T_{\min} = 213.0K$

$T_0 =$ starting temperature of calculation = $T_{a_{sun1}} > T_a$

$T_a =$ actual temperature

The constant c must be calculated for the sunlight phase with T_S=330K , c_s=2208 s and for eclipse, with T_E=213K and c_E=8213 s.

The values ε_A, m_i, c_w are the same like in chapter 2.7.
ε_A = average emissivity value for the satellite = 0.57 .

Following *Table 2-6* shows which temperature values are reached over a period of 3 orbits:

Instationary calculations							
Coverage (illuminated side)	Values	bottom 70% solar cells 30% aluminum			bottom 70% solar cells 30% black paint		
		1.Orbit	2.Orbit	3.Orbit	1.Orbit	2.Orbit	3.Orbit
70% solar cells 30% aluminum	T_S	314.0K	321.0K	321.2K	322.2K	326.3K	326.4K
	T_E	256.6K	251.9K	251.9K	259.8K	261.0K	261.0K
100% aluminum	T_S	279.9K	288.7K	289.4K	294.1K	299.8K	300.0K
	T_E	243.8K	247.5K	247.8K	251.0K	252.9K	253.0K
70% solar cells 30% black paint	T_S	286.5K	291.0K	291.1K	294.5K	297.2K	297.3K
	T_E	226.6K	227.8K	227.8K	229.8K	230.5K	230.5K
100% black paint	T_S	288.4K	292.7K	292.8K	296.2K	298.8K	298.9K
	T_E	227.1K	228.3K	228.3K	230.3K	231.0K	231.0K

Table 2-6 Results for the transient calculation with electrical power dissipation

- The results show that Compass-1 is too hot in the Sun phase when the sides are covered with aluminum and solar cells and the bottom is black painted and covered with solar cells. The temperature is with T_S=326.4K about 53°C above the battery temperature limit. To avoid such high temperatures Multi Layer Insulation (MLI) can be mounted instead of pure aluminum surface. If during the eclipse the temperature is still too cold, a heater will be used to ensure the allowable temperatures, minimum.

- The second alternative for the surface finish is the coverage with 70% solar cells and 30% black paint on all surfaces. In the Sun phase the temperatures are within the allowable subsystem temperature limits. But in the eclipse the temperatures are too cold. For this case a heater will be attached to the battery to maintain the operational cold limit. .

2.8. Calculations to avoid the extreme temperatures

2.8.1 Surface finish with MLI

In the following section the calculation for steady-state and transient temperatures will be restarted with the Multi Layer Insulation MLI (material properties are shown in *Table 2-7*). This is necessary for the case (results chapter 2.8), where the sides are covered with pure aluminum and solar cells, because the satellite is too hot during the Sun phase. For this reason new surface finish with MLI has been chosen, acting as radiation shield. MLI, also known as thermal blanketing, insulates the spacecraft by minimizing radiation input and heat absorption. A wide range of different MLI designs are existing, so a aluminum coated 3mil. Kapton foil has been chosen on Compass-1.

Case A: MLI protection

The MLI will be mounted on the top surface of Compass-1 which will be illuminated during the Sun phase. The bottom side will be covered with solar cells and black paint and the other sides are covered with solar cells/aluminum (*Figure 2-4*).

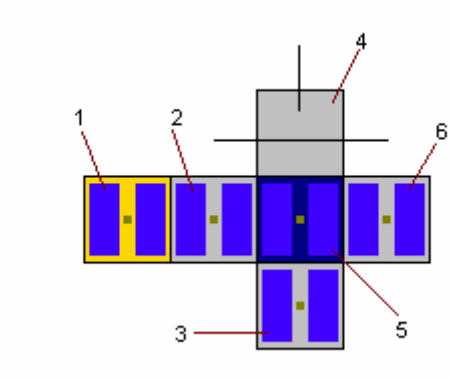

Figure 2-4 Structure with MLI and solar cells on top side

The computation according to chapter 2.5 “worst cases” and chapter 2.6 “Instationary calculation” are done with material properties shown in *Table 2-7*.

	MLI
Weight [g/m^2]	500
Conductivity [W/(m*K)]	0.02
Emissivity (thermal)	0.6
Absorptivity (solar)	0.15

Table 2-7 Material properties for MLI [7]

For the top side covered with MLI and solar cells the average values for the thermo-optical properties are:

$$\alpha_{Bp-Sc} = 0.7 \cdot 0.92 + 0.3 \cdot 0.15 = 0.689$$
$$\varepsilon_{Bp-Sc} = 0.7 \cdot 0.85 + 0.3 \cdot 0.6 = 0.775$$

ε_A = average emissivity value for the satellite = 0.7

$$\varepsilon^*_{IR} = \frac{3 \cdot \varepsilon_{Sc-Al} + 1 \cdot \varepsilon_{Al} + 1 \cdot \varepsilon_{Sc-MLI}}{5} = \frac{3 \cdot 0.62 + 0.08 + 0.775}{5} = 0.543$$

Using the equation (28) in chapter 2.5.1 and equation (29) in chapter 2.5.2 the equilibrium temperatures with internal power dissipation are:

* For the cold case at the end of eclipse: $T_{\min} = 210K$
* For the hot case in Sun: $T_{\max} = 323{,}3K$

With these conditions an instationary calculation for a period of 3 orbits has been done. The constant c for the heating up phase is c_{max}=1912.5 s, and for the cooling down phase c_{min}=6978.3 s. The results are shown below, in *Table 2-8*:

Coverage (illuminated side)	Values	bottom 70% solar cells 30% black paint		
		1.Orbit	2.Orbit	3.Orbit
70% solar cells 30% MLI	T_S	318.6K	320.8K	321.0K
	T_E	250.8K	251.0K	251.2K

Table 2-8 Instationary calculation results for MLI,(Case A)

Results:

The temperature for the worst hot case is still too high for the battery. It is not sufficient to cover only the top side with MLI, so that a new analysis will be done for coverage with mounted MLI on every side, except the bottom side which is orientated to the Earth.

Case B: MLI protection (all surfaces except the bottom side)

In this calculation on every side MLI will be mounted, except the bottom side, which keep painted black and covered with solar cells *(Figure 2-5)*

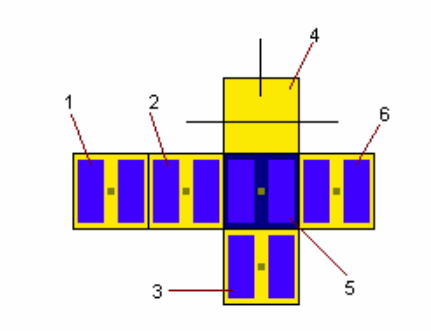

Figure 2-5 Structure with MLI and solar cells coverage

With $\varepsilon_{IR}^{*} = 0.74$ the equilibrium temperatures are:

* For the cold case at the end of eclipse: $T_{\min} = 194.3K$
* For the hot case in Sun: $T_{\max} = 304.3K$

Using the equation (34) in chapter 2.8.1 and equation (35) in chapter 2.8.2 a new instationary calculation with $c_{\min} = 1139s$ and $c_{\max} = 296.5s$ has been done.

Coverage (illuminated side)	Values	bottom 70% solar cells 30% black paint		
		1.Orbit	2.Orbit	3.Orbit
70% solar cells 30% MLI	T_S	304.3K	304.3K	304.3K
	T_E	194.3K	196.0K	196.0K

Table 2-9 Instationary calculation results for MLI, (Case B)

The results show that the application of MLI was a positive choice for the Sun period, but the temperature level dropped very deeply in the eclipse. The reason of this low temperature is the low absorptivity of MLI.

Case C: Heater attached to the battery

To maintain the satellite temperature above the operational cold limit during the eclipse an additional heater is required. Electrical resistance heaters are the best solution for providing heat for the spacecraft equipments. Currently 86mW have been allocated to the thermal subsystem as heating power. A detailed definition and selec-

tion of a heater is described in chapter 4 “Thermal control”. A new transient calculation will be done for the total time of eclipse, using a heater.

For the worst cold case with $\dot{Q}_{P_H} = 86mW$ the satellite has a new equilibrium temperature of:

$$T_{\min} = \left[T_{ambient}^4 + \frac{\dot{Q}_{P_H}}{\varepsilon_A \cdot A_{Sat} \cdot \sigma} \right]^{1/4} = 197.1K$$

$T_{ambient} = 196.0K$ is the ambient temperature inside the satellite at the end of eclipse after the 3rd orbit without a heater, (one node model)

$T_{\min} = T_E = 197.1K$ is the new temperature value for the instationary calculation

$T_o =$ starting temperature of calculation = 304.3K

The constant $c_{\min} = 198.2s$

At the end of eclipse with a switched on heater the temperature for the satellite is T=198.2K. The reasons for this low temperature are on the one hand, that the heater does not provide enough energy to heat the complete satellite during the eclipse. On the other hand the low absorptivity of MLI prevents the heat input during the Sun period. The temperature during the Sun period is slightly above the upper allowable temperature limit for battery. The results show that in this case the application of MLI has not turned out as a satisfactory solution.

2.9.2 Heater attached to battery

As herein above mentioned (in chapter 2.8, *Table 2-10*) there is an alternative solution (70% solar cells and 30% black paint on all surfaces) to maintain the temperature within the allowable limits.

This coverage is a sufficient solution for the Sun period T_{Sun} =297.3K. During the eclipse period (T_E=230.5K) it is required to attach a heater to the battery.

It is difficult to examine an exact temperature value which is actually present on the battery at the end of the eclipse using the equations from the section before. This equations based on the assumption of an one-node model and can be not used on a simple transformation for separate calculation of battery temperatures as a sub-node.

To find out how long and when a heater has to be switched on to hold the temperature limits, in the following chapter an electrical analysis is investigated by using the finite element method.

3 3-D model of Compass-1

The purpose of this chapter is to develop a thermal model which will simulate the Compass-1 temperature behavior for its normal orbit.

The nodal network modeling method first divides the satellite for thermal analysis into a finite number of nodes and connects between node and node by using thermal resistance. This method has advantages of simplicity and fast calculation.

3.1 Thermal model

The task of thermal modeling is the adequate consideration of Compass-1's geometry and thermal material properties as well as the formulation of appropriate initial and boundary conditions. This will describe the integration of the object in the physical environment on a proper way. The problem is to create a thermal model, which, is on the one hand simple enough to limit the expenditure and time needed for the simulation and which is, on the other hand, detailed enough to give an adequate description of the physical situation and relations.

In this analysis the ANSYS software has been chosen. The advantage one of Ansys is that it considers the material properties accurately and it allows working in three dimensional space.

Because the heat flow that radiation causes varies with the forth power of the body's absolute temperature, radiation analyses are highly nonlinear. An iterative solution is required to reach a converged solution.

The basis for thermal analysis in ANSYS is a heat balance equation obtained from the principle of conservation of energy. The finite element solution one performs via ANSYS calculates nodal temperatures, and then uses the nodal temperatures to obtain other thermal quantities.

For a 3D analysis a SHELL157 element was chosen with Radiosity Solver Method (RSM). For the Radiosity Solver Method SHELL157 must be superimposed on defined conditions for radiation. The RSM works for generalized radiation problems involving two or more surfaces receiving and emitting radiation. Appendix D gives a detailed program structure of the Radiosity Solver Method.

The thermal model was build with the Solid70 element. Solid70 has a three-dimensional thermal conduction capability. The element has eight nodes with a single degree of freedom, temperature, at each node [8]. The element is applicable to a three-dimensional, steady-state or transient thermal analysis. The element also can compensate for mass transported heat flow from a constant velocity field.

The geometry, node locations, and the coordinate system for this element are shown in *Figure 3-1*. The element is defined by eight nodes and the orthotropic material properties. Orthotropic material directions correspond to the element coordinate directions.

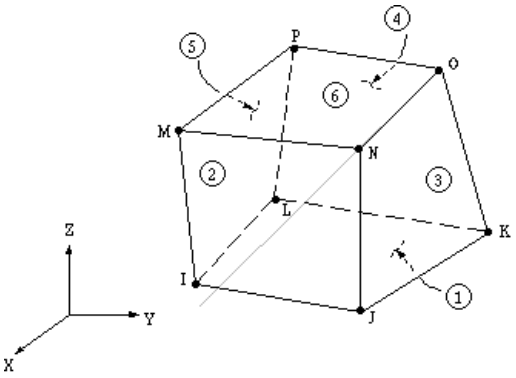

Figure 3-1 Solid Element

SHELL157 (*Figure 3-2)* is a 3-D element having in-plane thermal and electrical conduction capabilities. The element has four nodes with two degrees of freedom, temperature and voltage, at each node. The element applies to a 3-D, steady-state or transient thermal analysis, although the element includes no transient electrical capacitance or inductance effects. The element requires an iterative solution to include the Joule heating effect in the thermal solution.

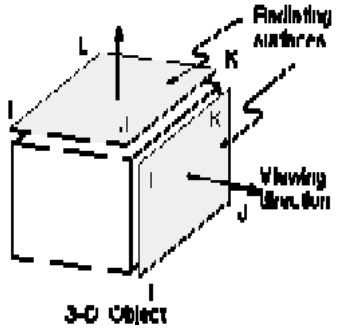

Figure 3-2 SHELL57 Thermal Shell

The major heat input for the Compass-1 model is the solar flux. Earth's IR radiation and the Sun radiation reflected by the Earth's atmosphere (Albedo) will also have a significant contribution to the thermal behavior. There is also a heat dissipation from the electronics, inside the satellite. The energy output is only by radiation to space background. The amount of absorbed and emitted heat will be regulated by the optical surface properties.

3.2 Analysis

The aim of the thermal analysis is to determine with a good accuracy the temperature mapping of Compass-1 and then develop a thermal control solution to maintain all components within their allowable temperature limits for all operating modes (*Table 1-1).*

ANSYS supports two types of thermal analysis:

1. A steady-state thermal analysis determines the temperature distribution and other thermal quantities under steady-state loading conditions. A steady-state loading condition is a situation where heat storage effects varying over a period of time can be ignored.

2. A transient thermal analysis determines the temperature distribution and other thermal quantities under conditions that vary over a period of time.

The model was created as a cube of aluminum with a wall thickness of 1 mm as defined by the structures group with previously given optical surface properties.
This model consists of the outer structure (*Figure 3-3)* and the main board and battery (*Figure 3-4)*, internals.

Due to the calculations in chapter 2, in this section the following case was analyzed: 5 surfaces covered with 30% black paint and 70% solar cells, one side, where the antennas are mounted is painted black.

For the analysis the model was simplified: the emissivity was scaled according to the percentage of the area occupied on each side by solar cells and raw aluminum, the density, the thickness and the specific heat have been summarized in percent.

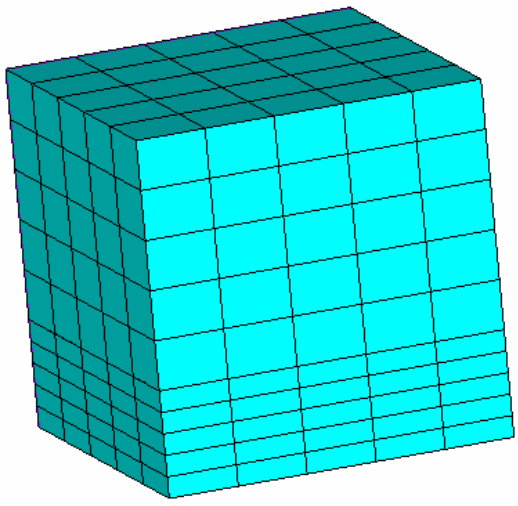

Figure 3-3 Finite element model

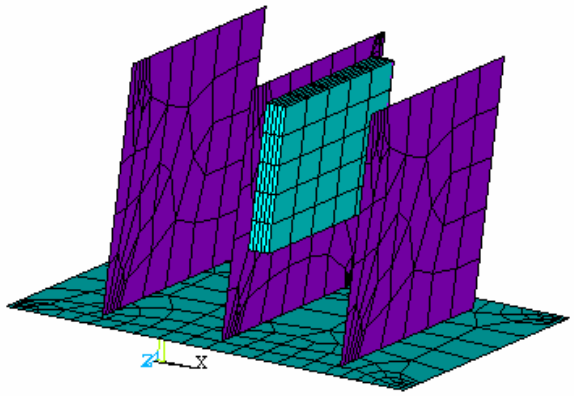

Figure 3-4 Components of the finite element model inside

For an accurate thermal analysis the model requires the identification of heat sources and sinks, external and internal, such as heater. The transient analysis is carried out in two phases: Sun phase and eclipse.
The first analyses are done with internal power dissipation 1W and without internal heat from heater.

In the Sun phase, with duration of t_{sun}=60.5min there are heat flux loads from the Sun, Albedo and the Earth. A bulk temperature of 3 K was defined to simulate the background temperature, which surrounds Compass-1 in space. The load values are given in *Table 3-1.* The Sun flux is loaded on the top of Compass-1, Albedo and Earth radiation on the bottom. This case exists when β=0 (β= angle between the Sun vector and the orbit plane, chapter 1.2).

Input parameters	
Heat flux Sun	1370 W/m²
Albedo	470 W/m²
IR radiation	198 W/m² [4)]
Time (per orbit)	3600 s

Table 3-1 Heat input Parameters

●Sun phase calculation

The transient temperature calculation of the outer skin for the Sun phase Compass-1 after the 3rd orbit is shown in *Figure 3-5*. The temperature values are between 11.8°C and 18.22 °C for the surface of the satellite.

Figure 3-6 shows the temperature values inside Compass-1. The results show that the temperature values are within the allowable limits for each satellite component.

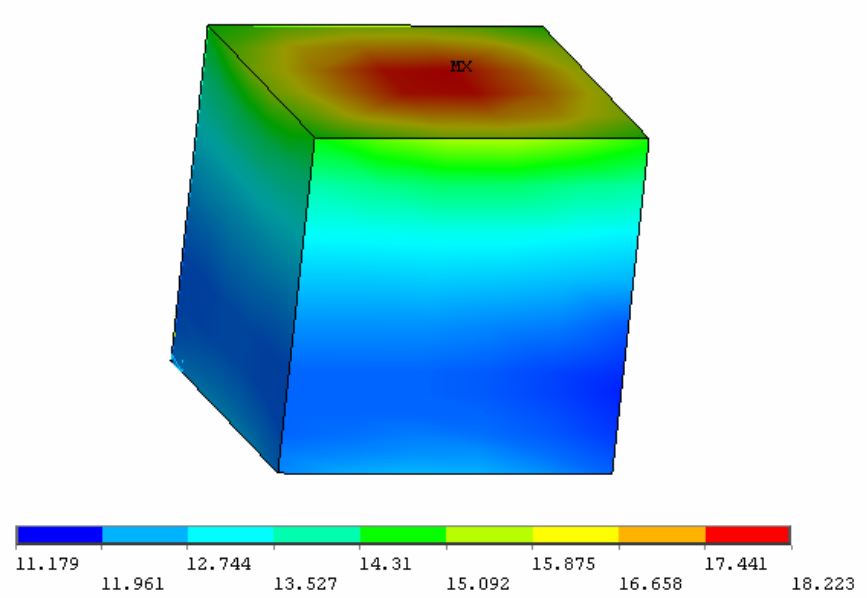

Figure 3-5 Temperature distribution at the end of Sun phase

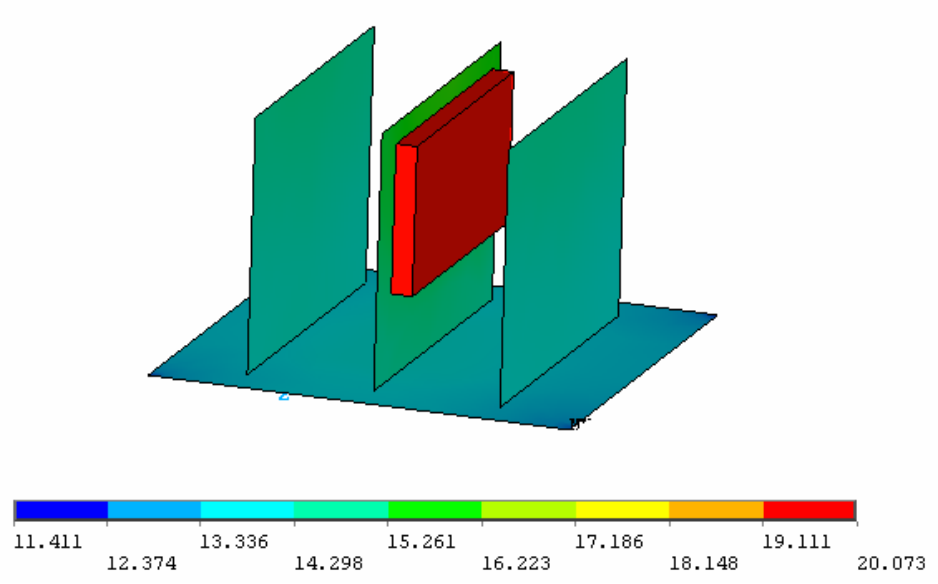

Figure 3-6 Temperature distribution inside at the end of Sun phase

●Shadow phase calculation

After the Sun phase the eclipse was carried out with $t_{eclipse}$ =35.5min. The only load is the Earth IR I_E=198 W/m² [4)] applied on the bottom side of Compass-1. In *Figure 3-7* the temperature contour on outer skin of Compass-1 in eclipse can be seen. The temperature values are between -43.5°C and -41.7°C. The results shown in *Figure 3-8* indicate that the temperature values are between -9.8°C and -43.4°C. Comparing this to the operating temperature limits of Compass-1, a heater is needed to protect the battery.

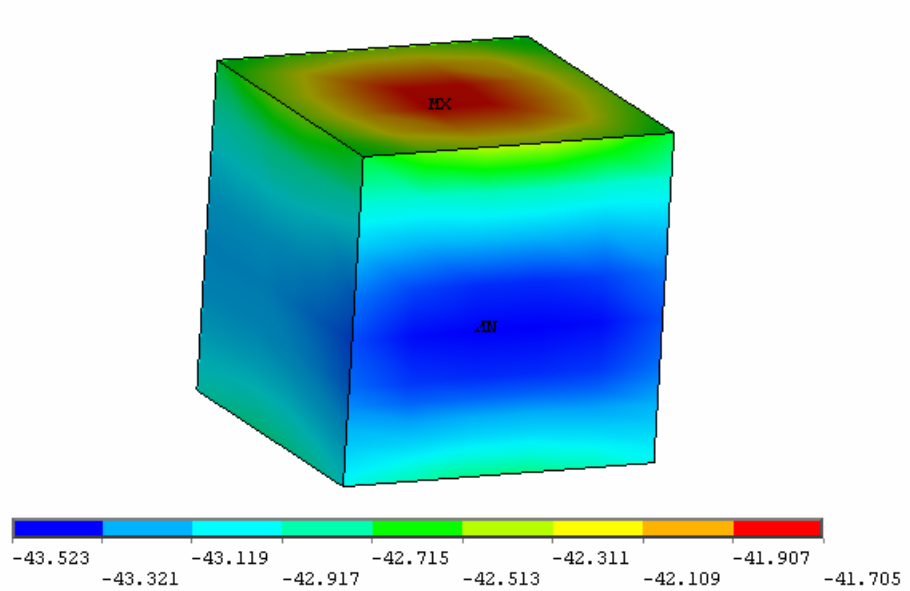

Figure 3-7 Temperature distribution on outer structure for shadow phase

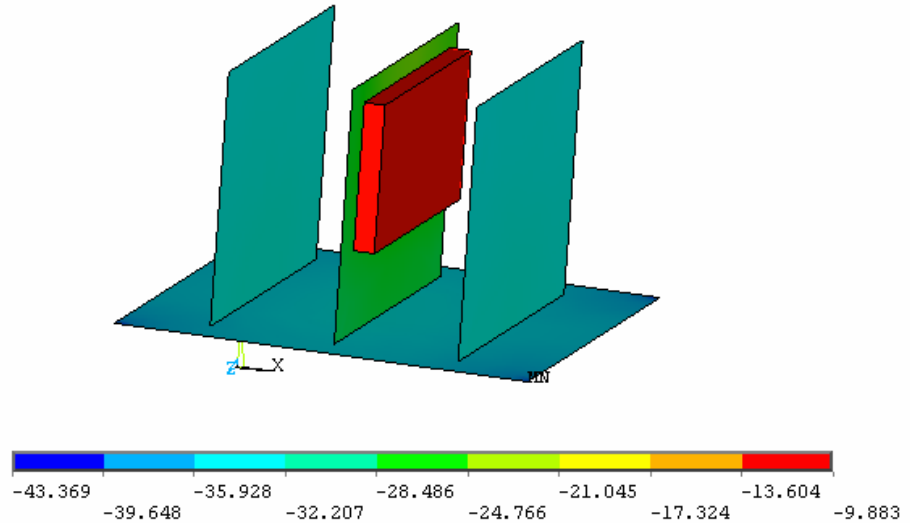

Figure 3-8 Temperature distribution inside Compass-1 at the end of the shadow phase

●Shadow phase with heater

The further analysis was done to determine how long the heater attached to the battery has to be switch on. Several analyses with different conditions (i.e. time and power the heater was switched on) have been done. *Figure 3-9* shows the optimum results inside Compass-1 when the heater is on. Chapter 3.3 describes the conditions of this analysis, in detail

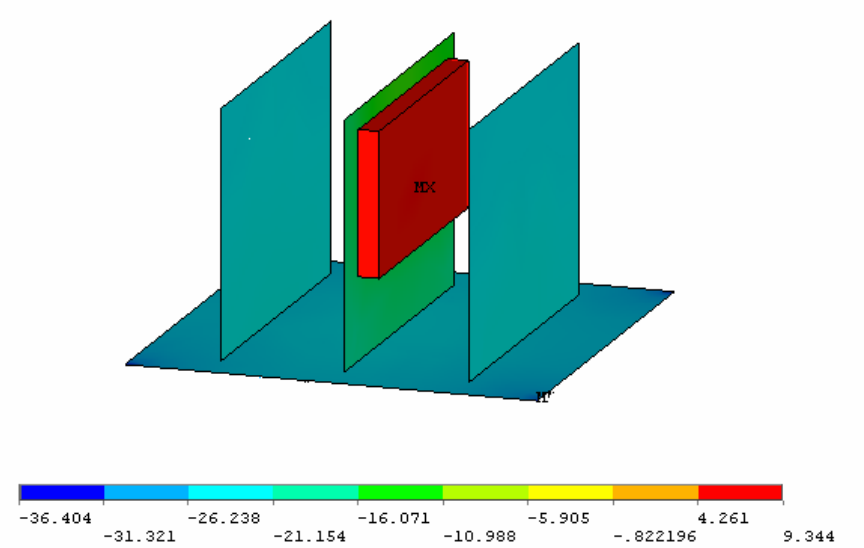

Figure 3-9 Temperature distribution during eclipse when heater was attached to the battery

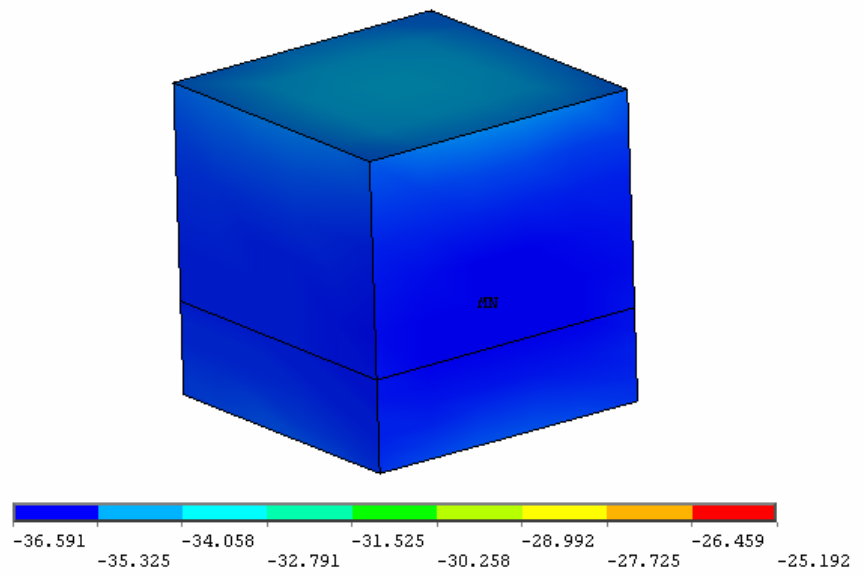

Figure 3-10 Temperature distribution during eclipse with heater

3.3 Nodal network modeling results

From the transient analysis of the nodal network modeling with ANSYS, it was obtained that the maximum temperature is expected between 11.1°C, inside Compass-1 and 18.2°C on outer skin during the Sun period. The temperature contour which results from the thermal analysis in Sun phase is shown in *Figure 3-5* and Figure *3-6*. It indicates that the temperatures are within the upper temperature limits.

The temperature distribution during eclipse is shown in *Figure 3-7* and *Figure 3-8*. The average temperature values are between -43.9°C and -9.88°C.

Due to the limited temperature ranges of the electronic components within the satellite, especially the battery, it is necessary to control the temperature during the eclipse period. The battery is the most thermally sensitive one of the satellite subsystems, because it cannot operate below 5°C and above 20°C.

Figure 3-9 shows results for an analysis which was done when the heater was switched on.

After different analyses following solution is sufficient: At the end of the Sun phase, when Compass-1 is enters the shadow, five minutes later the heater has to be switched on with a power of 42mW. The temperature of the battery is an average of 7°C, which is a perfect value within the operational limits. When Compass-1 is about t=11.67min in the shadow, the heater has to increase its power up to 86mW and has to keep this power to the end of the eclipse. The temperature distribution is shown in *Figure 3-9* at the end of the shadow phase.

The temperatures at the electronics component are between -31.3°C and -21.15°C. Comparing the operational temperature limits (*Table 1-1)* the values are within their allowable limits.

Contrary to the battery the structure (outer skin) is still very cold. The temperature values for the structure are shown in *Figure 3-10.* The values are between -36.5°C and -26.5°C. These values are also within their operational limits.

4 Thermal Control

It is necessary to keep the temperature of Compass-1 in a defined temperature range during its entire mission, because all electronic devices are designed to operate in this temperature range. Basically, the allowable temperature range is defined by the “weakest” subsystem component, i.e. the component with the smallest temperature range.

The thermal control system is composed of two different types of systems the passive and active. The passive is generally lighter, requires less electrical power and is less costly then an active design. The active systems are used for manned spacecraft, for situations requiring very close tolerance temperature control or for components that dissipate a large amount of waste energy. A completely passive system is not sufficient for Compass-1. The spacecraft will carry a combination of passive and active solutions.

4.1 Active thermal control system

The active thermal control of a spacecraft may require the use of heaters, cooler, shutters, louvers or cryogenic materials. The heaters are usually wire-wound resistance heaters that may be controlled by a thermostat. Shutters and louvers are the most common active thermal control devices. The louvers open when heat needs to be radiated and close when the temperature is lowered. For long term cooling to low temperatures, the best approach is to use the cryogenic fluid because it uses less energy and it is more effective.

A comparison between the analysis results above and the temperature limits listed in *Table 1-1,* chapter 1, shows that the thermal environment is not suitable for the battery and camera components without thermal management efforts. In the worst cold case the components will excessively cool and perhaps cease to function. To prevent that, one heater will be attached to the battery and activated each time, the temperature drops below a certain threshold level.

4.2 Passive thermal control system

The techniques applied for passive thermal control include the use of spacecraft coatings, insulation blankets (MLI), Sun shields, radiating fins and heat pipes. Due to

the volume and power constrains of Compass-1, passive control methods in the form of thermal coatings and insulation are preferred.

Thermal finishes are the simplest solution. They can vary greatly in type. Most are simple paints that can be applied to the surface of a spacecraft structure. Thermal finishes include paints, silverized plastics and coatings.

Generally, high emittance is desirable so that internally generated heat can be radiated effectively and low absorptivity is desirable to minimize the effects of solar radiation.

Multi Layers Insulation is used to insulate the inside of the satellite from its external environment and prevent excessive heat loss from a component or excessive heating. Conductive heat transfer is practically eliminated; heat transfer across this material is primarily by thermal radiation from one layer to the next. MLI consists typically of several layers of aluminized Mylar or Kapton films with a low conductance spacer.

The operating ranges of different components of Compass-1 drive the thermal requirements, as well as the power dissipated and exposure to the external environment. *Table 1-1* in chapter 1.1 shows the thermal operating ranges for the vital components on Compass-1. Out of these components, the camera and the battery are the most thermally constrained.

The bottom side of the satellite will be painted black, because of the high absorptivity. There are also two solar cells on the bottom panel, which converts the Albedo (after all 35% of the solar flux) radiation to electrical energy. The top of the satellite and the side plates are made from aluminum (6061-T6), which will be also painted black and are covered with two solar cells each, apart from the antenna side.

Hardware

To avoid the low temperatures during the eclipse the implementation of heaters has been found an adequate solution. The heaters can be hard or flexible. Flexible heaters are the most common in satellites because they can conform to various shapes. Heater from Minco Products, Inc *(Figure4-1)* offers a wide range of different heaters, but some are not suitable for the given constrains. Wire-wound rubber heaters are more economical in larger size, oversized for our size requirements. Silicone heaters are not suitable for radiation and vacuum. Mica heaters consist of an etched foil element sandwiched between layers of mica and they are not flexible. A Kapton has been selected. Kapton is a thin, semitransparent material with excellent dielectric strength. Kapton heaters are ideal for applications with space and weight limitations, or where the heater will be exposed to vacuum.

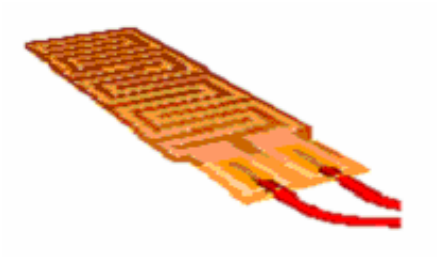

Figure 4-1 Heater

The heater will heat the battery during the eclipse to within the required temperature range for that component. The heater will be connected to the electrical power subsystem (EPS) and is closed-loop controlled by a temperature sensor via Command and Data Handling System (CDHS). It constantly measures the current temperature and controls the heater's value setting to increase or decrease Compass-1 temperature according the defined setting. The heater is switched on, when the actual temperature T_a is lower than the required temperature T_{rmin}=5°C. If the actual temperature T_a is higher than the required temperature T_{rmax}=20°C is higher the heater shall switch off. The block diagram in *Figure 4-4* shows the closed-loop for the heater [R16].

Minco Products, Inc – Strip heater with Kapton Insulation	
Product number	HK 5447 R290 L12 E
Mass	0.4g
Resistance	290 Ω
Power	86m W
Volume	63.5 x 76.2 x .127mm
Location	inside top of battery box

Table 4-1 Heater characteristics

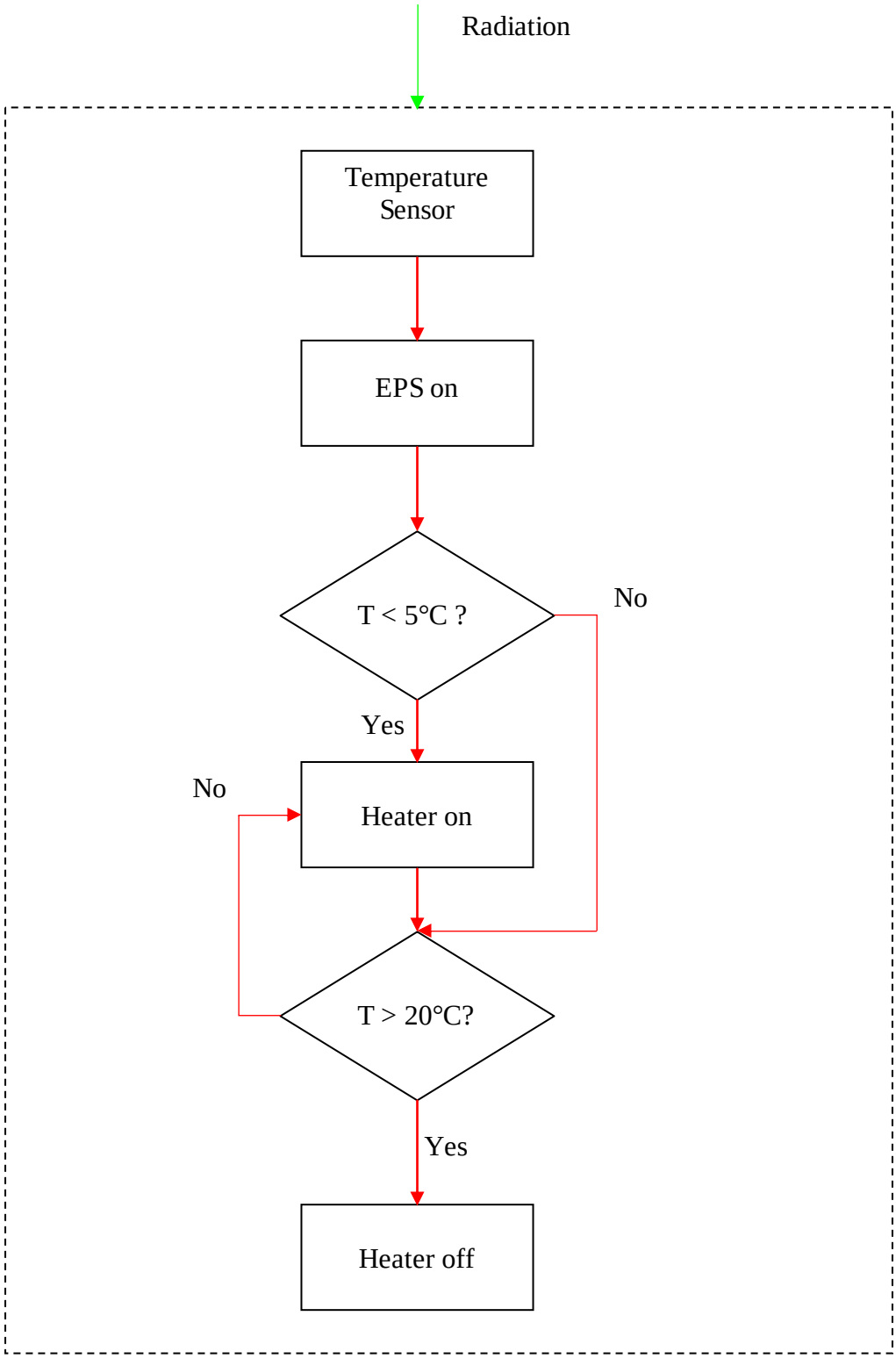

Figure 4-2 Thermal subsystem block diagram

Temperature Sensors:

Temperature sensors are used to relay relevant thermal information to EPS, which toggles the thermal controls. The heater shall be turned on or off based on the instruction by the EPS.

The LM75 is a temperature sensor (*Figure4-3*), Delta-Sigma analog-to-digital converter, and digital over-temperature detector with I²C® interface. The host can query the LM75 at any time to read the temperature. The open-drain Overtemperature Shutdown (O.S.) output becomes active when the temperature exceeds a programmable limit. This pin can operate in either “Comparator” or “Interrupt” mode.

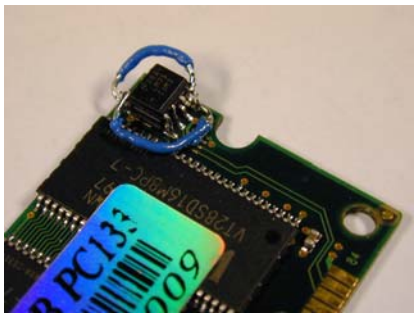

Figure 4-3 Lm75 Temperature Sensor

The LM75 sensors will be installed on all boards inside of the satellite, to the camera and to the battery of the power subsystem. The purpose is to measure the temperature of each board of the satellite and to measure the temperature of the battery and send the information to EPS to make sure the temperatures are within their survival limits [R14]

Temperature sensors shall be connected to a 2-wire bus.

LM75 Temperature sensor	
Supply voltage	3.0V to 5.5V
Supply current	operating 250µA (typ); 1mA (max) shutdown 4µA (typ)
Temperature	-25°C to +100°C
Accuracy	± 2°C (max)
Temperature	-55°C to +125°C
Accuracy	± 3°C (max)
Interface	I²C Bus

Table 4-2 Temperature sensor LM75 characteristics

The second temperature sensor M-FK 222 (*Figure 4*-3)is used to determine the Solar Cell temperature on each side of the spacecraft. This platinium thin-film sensor is small and light and can be used an a teperature range from –70°C – 500°C. There is very long-term stable wit a drift of 0.04% after 1000h at 500°C [R15].

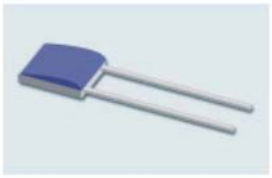

Figure 4-3 M-FK 222 Temperature Sensor

M-FK 222 Temperature sensor	
Insulation resistance	> 10 MΩ at 20°C > 1MΩ at 500°C
Temperature range	-70°C to +500°C
Temperature coefficient	TCR=3850 ppmK
Leads	Nickel platinum-clad wire
Measuring current	100Ω: 0.1 to 0.3mA

Table 4-3 Temperature sensor M-FK 222 characteristics

4.3 System optimization

The results of the previous calculations and the analysis show, the overall temperature of Compass-1 is too low to fulfill the requirements. From the numbers can be derived that Compass-1 tends towards lower temperatures rather than higher. To maintain the satellite at a mean temperature close to 20°C, a satisfactory balance has to be achieved between heat sources and cold sinks. There is a variety of engineering parameters that can be adjusted in order to achieve this goal. However, only few of those are open for change. As an example, changing the geometry of the spacecraft can have a positive effect on the temperatures of Compass-1. For obvious reasons, changing the geometrical configuration is not an option.

Another way of passively improving the thermal behavior of the spacecraft is to influence its radiation characteristics. These are governed by its surface properties, in particular ε and α. As has been discussed earlier, a black paint coating of exposed aluminum parts has been assumed during the calculations. This coating generally leads to higher temperatures. The selection of coating is an optimum solution and will not be adjusted.

The bottom line problem is that the satellite will cool down to exceedingly low temperatures during cold mission phases, i.e. phases without significant energy intake. The active solution is to keep Compass-1 warm by electrical heaters during these phases. The EPS manages the thermal control system. Temperature measurements recorded by a network of temperature sensors are compared to reference values.

5 Conclusion

Spacecraft components must be maintained within their acceptable temperature limits in order to remain operational. Because of the low available thermal power it was a goal to provide an adequate control. Ideally, the thermal system would be as passive as possible to minimize mass and power requirements. Compass-1 will preliminary use coating and paints to control heat radiation. Special care was taken to ensure the allowable temperature limits. By comparing the analysis results to the temperature requirements of the components in *Figure 3-5* → *Figure 3-8* it is found that the temperature values during the Sun phase are within the allowable limits. For Compass-1 black paint on aluminum was chosen. In the eclipse the temperature for the battery is below the operating temperature limits. Therefore during the coldest scenario, the addition of 86mW of heater power is needed to maintain the battery in its operating status. A further analysis has been done with a heater to determinate a solution for the shadow phase. It is necessary to heat the satellite almost during the entire eclipse. But then the temperature values, especially the battery, stay within their operational temperature limits.

For the further work it would be recommended to perform thermal balance and thermal cycle tests. Compass-1 model, along with the other subsystems must be exposed to the high temperature and vacuum extreme in order to simulate the satellite in orbit.

6 References

[1] Willi Hallmann, Wilfried Ley (1999) *Handbuch Raumfahrttechnik*, Hanser

[2] Gilmore,David G. (1994) *Thermal Control Handbook*, The Aerospace Corporation Press, El Segundo, California

[3] Larson, W.J. and Wertz, J.R. (1996) *Space Mission Analysis and Design*. Kluwer Academic Publishers, Dordrecht, The Netherlands

[4] Siegal, R. and Howell, J. R., Thermal Radiation Heat Transfer, Second Edition, Hemisphere Publishing Corporation (1981)

[5] E.Messerschmid, S. Fasoulas (2000) *Raumfahrtsysteme*

[6] Glass, M.W., "Chaparral - A library package for solving large enclosure radiation heat transfer problems", Sandia National Laboratories, Albuquerque, NM (1995)

[7] Cohen, M.F. and Greenberg, D.P., "The Hemi-Cube: A Radiosity Solution for Complex Environments", Computer Graphics, Vol. 19, No. 3, pp. 31-40 (1985).

[8] Ansys Tutorial, Release 8.0

[9] ERNO/MBB AD18 Part4 Material properties

[10] Spectrolab, Material properties, www.spectrolab.com

[11] Suedahl, “Thermal Control Material & Metalized Films”

[12] www.**cubesat**.auc.dk/documents/psu/Chapter5.pdf

[13] http://www.lrt.mw.tum.de/lehrbetrieb

[14] www.national.com/pf/LM/LM75.html

[15] www.a**m**itra.fi/enews1.ht**m**l

[16] www.minco.com

Appendix A

Following detailed instationary calculations for different cases with various surface properties are presented:

Calculation for illuminated coverage (the bottom either) with 70% solar cells and 30% aluminum

The equilibrium temperatures are:

* For the cold case at the end of eclipse: $T_{\min} = 177.0K$
* For the hot case in Sun: $T_{\max} = 320.8K$

Using the equation (27) for the heating up phase, where

$T_S = T_{\max}$ = 320.8K
$T_o =$ starting temperature of calculation = 177.0K

and equation (28) for cooling down, where

$T_E = T_{\min}$ = 177.0K
$T_o =$ starting temperature of calculation = $T_{a_{sun1}} > T_a$

with the constant $c_S = 2585s$ and $c_E = 15392s$

T_S = 320.8K , T_E = 177.0K

ε_A = average emissivity value for the satellite = 0.53

$$\dot{Q}_A = 4 \cdot \dot{Q}_{Al-Sc} + 1 \cdot \dot{Q}_{Bp-Sc} + 1 \cdot \dot{Q}_{Al}$$
$$\varepsilon_A \sigma T^4 A_T = \sigma T^4 (5A \cdot \varepsilon_{Al-Sc} + 1A \cdot \varepsilon_{Al})$$
$$\varepsilon_A = \frac{5}{6} \cdot \varepsilon_{Al-Sc} + \frac{1}{6} \cdot \varepsilon_{Al} = 0.53$$

Calculation for illuminated side coverage with 100% aluminum and black painted bottom with solar cells, orientated to Earth

The equilibrium temperatures are:

* For the cold case at the end of eclipse: $T_{\min} = 192.4K$
* For the hot case in Sun: $T_{\max} = 295.0K$

Using the equation (27) for the heating up phase, where

$T_S = T_{\max}$ = 295.0K
$T_o =$ starting temperature of calculation = 192.4K

and equation (28) for cooling down, where

$T_E = T_{\min}$ = 192.4K
$T_o =$ starting temperature of calculation = $T_{a_{sun1}} > T_a$

with the constant $c_S = 3091s$ and $c_E = 11143s$

T_S = 249.4K , T_E = 187.4K
ε_A = average emissivity value for the satellite = 0.57

Calculation for illuminated coverage with 100% aluminum and bottom side with 70% solar cells and 30% aluminum

The equilibrium temperatures are:

* For the cold case at the end of eclipse: $T_{\min} = 177.0K$
* For the hot case in Sun: $T_{\max} = 289.2K$

Using the equation (27) for the heating up phase, where

$T_S = T_{\max}$ = 289.2K
$T_o =$ starting temperature of calculation = 177.0K

and equation (28) for cooling down, where

$T_E = T_{\min}$ = 177.0K

$T_o =$ starting temperature of calculation = $T_{a_{sun1}} > T_a$

with the constant $c_S = 3529s$ and $c_E = 15392s$

T_S = 289.2K , T_E = 177.0K

ε_A = average emissivity value for the satellite = 0.53

Calculation for illuminated and orientated side to the Earth coverage with 70% solar cells and 30% black paint (illuminated side 4 covered with 100% black paint)

* For the cold case in the eclipse: $T_{\min} = 167.7K$
* For the hot case in Sun: $T_{\max} = 287.9K$

Using the equation (27) for the heating up phase, where

$T_S = T_{\max}$ = 287.9K

$T_o =$ starting temperature of calculation = 167.7K

and equation (28) for cooling down, where

$T_E = T_{\min}$ = 167.7K

$T_o =$ starting temperature of calculation = $T_{a_{sun1}} > T_a$

with the constant $c_S = 2179s$ and $c_E = 11025s$

T_S = 287.9K , T_E = 167.7K

m_{Al} = 270g and $c_{w_{Al}} = 980 \frac{Nm}{kg \cdot K}$

m_{SC} = 27g and $c_{w_{SC}} = 1600 \frac{Nm}{kg \cdot K}$

ε_A = average emissivity value for the satellite

$$\dot{Q}_A = 5 \cdot \dot{Q}_{Bp-Sc} + 1 \cdot \dot{Q}_{Bp}$$

$$\varepsilon_A \sigma T^4 A_T = \sigma T^4 (5A \cdot \varepsilon_{Bp-Sc} + 1A \cdot \varepsilon_{Bp})$$

$$\varepsilon_A = \frac{5}{6} \cdot \varepsilon_{Bp-Sc} + \frac{1}{6} \cdot \varepsilon_{Bp} = 0.87$$

Calculation for illuminated coverage with 70% solar cells and 30% black paint and the bottom coverage with 70% solar cells and 30% aluminum (illuminated side 4 covered with 100% black paint)

The equilibrium temperatures are:

* For the cold case in the eclipse: $T_{\min} = 154.4K$
* For the hot case in Sun: $T_{\max} = 290.3K$

Using the equation (27) for the heating up phase, where

$T_S = T_{\max}$ = 290.3K
$T_o =$ starting temperature of calculation = 154.4K

and equation (28) for cooling down, where

$T_E = T_{\min}$ = 154.4K
$T_o =$ starting temperature of calculation = $T_{a_{sun1}} > T_a$

with the constant $c_S = 2228s$ and $c_E = 14808\ s$

T_S = 290.3K , T_E = 154.4K
m_{Al} = 270g and $c_{w_{Al}} = 980\frac{Nm}{kg \cdot K}$
m_{SC} = 27g and $c_{w_{SC}} = 1600\frac{Nm}{kg \cdot K}$
ε_A = average emissivity value for the satellite

$$\dot{Q}_A = 4 \cdot \dot{Q}_{Bp-Sc} + 1 \cdot \dot{Q}_{Bp} + 1 \cdot \dot{Q}_{Al-Sc}$$
$$\varepsilon_A \sigma T^4 A_T = \sigma T^4 (4A \cdot \varepsilon_{Bp-Sc} + 1A \cdot \varepsilon_{Bp} + 1A \cdot \varepsilon_{Al-Sc})$$
$$\varepsilon_A = \frac{4}{6} \cdot \varepsilon_{Bp-Sc} + \frac{1}{6} \cdot \varepsilon_{Bp} + \frac{1}{6} \cdot \varepsilon_{Al-Sc} = 0.83$$

Calculation for illuminated side with 100% black paint and orientated bottom side with 70% solar cells and 30% aluminum

The equilibrium temperatures are:

* For the cold case in the eclipse: $T_{\min} = 154.4K$
* For the hot case in Sun: $T_{\max} = 286.1K$

Using the equation (27) for the heating up phase, where

$T_S = T_{\max}$ = 286.1K
$T_o =$ starting temperature of calculation = 154.4K

and equation (28) for cooling down, where

$T_E = T_{\min}$ = 154.4K
$T_o =$ starting temperature of calculation = $T_{a_{sun1}} > T_a$

with the constant $c_S = 2327s$ and $c_E = 14808s$

where

T_S = 286.1K , T_E = 154.4K
ε_A = average emissivity value for the satellite = 0.83

Calculation for illuminated side with 100% black paint and orientated side to Earth covered with 70% solar cells and 30% black paint

The equilibrium temperatures are:

* For the cold case in the eclipse: $T_{\min} = 167.7K$
* For the hot case in Sun: $T_{\max} = 289.6K$

Using the equation (27) for the heating up phase, where

$T_S = T_{\max}$ = 289.6K
$T_o =$ starting temperature of calculation = 167.7K

and equation (28) for cooling down, where

$T_E = T_{\min}$ = 167.7K

$T_o =$ starting temperature of calculation = $T_{a_{sun1}} > T_a$

with the constant $c_S = 2140s$ and $c_E = 11025s$

where

T_S = 289.6K , T_E = 167.7K

ε_A = average emissivity value for the satellite = 0.87

Appendix B

Following detailed instationary calculations (with internal power dissipation) for different cases with various surface properties are presented:

Calculation for coverage (the bottom either) with 70% solar cells and 30% aluminum

The equilibrium temperatures are:

* For the cold case at the end of eclipse: $T_{\min} = 202.2K$
* For the hot case in Sun: $T_{\max} = 326.0K$

Using the equation (27) for the heating up phase, where

$T_S = T_{\max}$ = 326.0K
$T_o =$ starting temperature of calculation = 202.2K

and equation (28) for cooling down, where

$T_E = T_{\min}$ = 202.2K
$T_o =$ starting temperature of calculation = $T_{a_{sun1}} > T_a$

with the constant $c_S = 2463.6s$ and $c_E = 10324.8s$

T_S = 326.0K , T_E = 202.2K
m_{Al} = 270g and $c_{w_{Al}} = 980\frac{Nm}{kg \cdot K}$
m_{SC} = 27g and $c_{w_{SC}} = 1600\frac{Nm}{kg \cdot K}$
ε_A = average emissivity value for the satellite = 0.53

Calculation for coverage with 100% aluminum and black painted bottom with solar cells

The equilibrium temperatures are:

* For the cold case at the end of eclipse: $T_{\min} = 213.0K$
* For the hot case in Sun: $T_{\max} = 305.0K$

Using the equation (27) for the heating up phase, where

$T_S = T_{\max}$ = 305.0K
$T_o =$ starting temperature of calculation = 213.0K

and equation (28) for cooling down, where

$T_E = T_{\min}$ = 213.0K
$T_o =$ starting temperature of calculation = $T_{a_{sun1}} > T_a$

with the constant $c_S = 2797s$ and $c_E = 8213s$

T_S = 305.0K , T_E = 213.0K
ε_A = average emissivity value for the satellite = 0.57

Calculation for illuminated coverage with 100% aluminum and bottom side with 70% solar cells and 30% aluminum

The equilibrium temperatures are:

* For the cold case at the end of eclipse: $T_{\min} = 202.2K$
* For the hot case in Sun: $T_{\max} = 296.1K$

Using the equation (27) for the heating up phase, where

$T_S = T_{\max}$ = 296.1K
$T_o =$ starting temperature of calculation = 202.2K

and equation (28) for cooling down, where

$T_E = T_{\min}$ = 202.2K
$T_o =$ starting temperature of calculation = $T_{a_{sun1}} > T_a$

with the constant $c_S = 3288s$ and $c_E = 10324s$

T_S = 296.1K , T_E = 202.2K
ε_A = average emissivity value for the satellite = 0.53

Calculation for illuminated and orientated side to the Earth coverage with 70% solar cells and 30% black paint

* For the cold case in the eclipse: $T_{\min} = 185.7K$
* For the hot case in Sun: $T_{\max} = 299.6K$

Using the equation (27) for the heating up phase, where

$T_S = T_{\max}$ = 299.6K
$T_o =$ starting temperature of calculation = 185.7K

and equation (28) for cooling down, where

$T_E = T_{\min}$ = 185.7K
$T_o =$ starting temperature of calculation = $T_{a_{sun1}} > T_a$

with the constant $c_S = 1934s$ and $c_E = 8120s$

T_S = 299.6K , T_E = 185.7K
ε_A = average emissivity value for the satellite $= 0.87$

Calculation for illuminated coverage with 70% solar cells and 30% black paint and the bottom coverage with 70% solar cells and 30% aluminum

The equilibrium temperatures are:

* For the cold case in the eclipse: $T_{\min} = 176.3K$
* For the hot case in Sun: $T_{\max} = 294.3K$

Using the equation (27) for the heating up phase, where

$T_S = T_{\max}$ = 294.3K
$T_o =$ starting temperature of calculation = 176.3K

and equation (28) for cooling down, where

$T_E = T_{\min}$ = 176.3K
$T_o =$ starting temperature of calculation = $T_{a_{sun1}} > T_a$

with the constant $c_S = 2138s$ and $c_E = 9946s$

T_S = 294.3K , T_E = 176.3K
ε_A = average emissivity value for the satellite $= 0.83$

Calculation for illuminated side covered with 100% black paint and bottom side with 70% solar cells and 30% aluminum

The equilibrium temperatures are:

* For the cold case in the eclipse: $T_{\min} = 176.3K$
* For the hot case in Sun: $T_{\max} = 295.9K$

Using the equation (27) for the heating up phase, where

$T_S = T_{\max}$ = 295.9K
$T_o =$ starting temperature of calculation = 176.3K

and equation (28) for cooling down, where

$T_E = T_{\min}$ = 176.3K
$T_o =$ starting temperature of calculation = $T_{a_{sun1}} > T_a$

with the constant $c_S = 2104s$ and $c_E = 9946s$

where

T_S = 295.9K , T_E = 176.3K
ε_A = average emissivity value for the satellite = 0.83

Calculation for coverage with 100% black paint and bottom side with 70% solar cells and 30% black paint

The equilibrium temperatures are:

* For the cold case in the eclipse: $T_{\min} = 185.7K$
* For the hot case in Sun: $T_{\max} = 301.1K$

Using the equation (27) for the heating up phase, where

$T_S = T_{\max}$ = 301.1K
$T_o =$ starting temperature of calculation = 185.7K

and equation (28) for cooling down, where

$T_E = T_{\min}$ = 185.7K
$T_o =$ starting temperature of calculation = $T_{a_{sun1}} > T_a$

with the constant $c_S = 1905s$ and $c_E = 8120s$

where

T_S = 301.1K , T_E = 185.7K
ε_A = average emissivity value for the satellite = 0.87

Appendix C

This section shows the transient analysis results for a case if the satellite is covered with 70% solar cells and 30% aluminum, one side with 100% aluminum and bottom side with 70% solar cells and 30% black paint.

The analysis for the Sun period is computed using a solar flux of 1370 W/m², Albedo flux equal to 0.34 the solar flux and the Earth infrared flux of 198W/m² (the ρ =angular radius of the Earth was considered).The eclipse period has only Earth infrared flux.

Figure 6-1 shows the temperature distribution in the Sun phase. The values are above the allowable temperature limits for the battery.

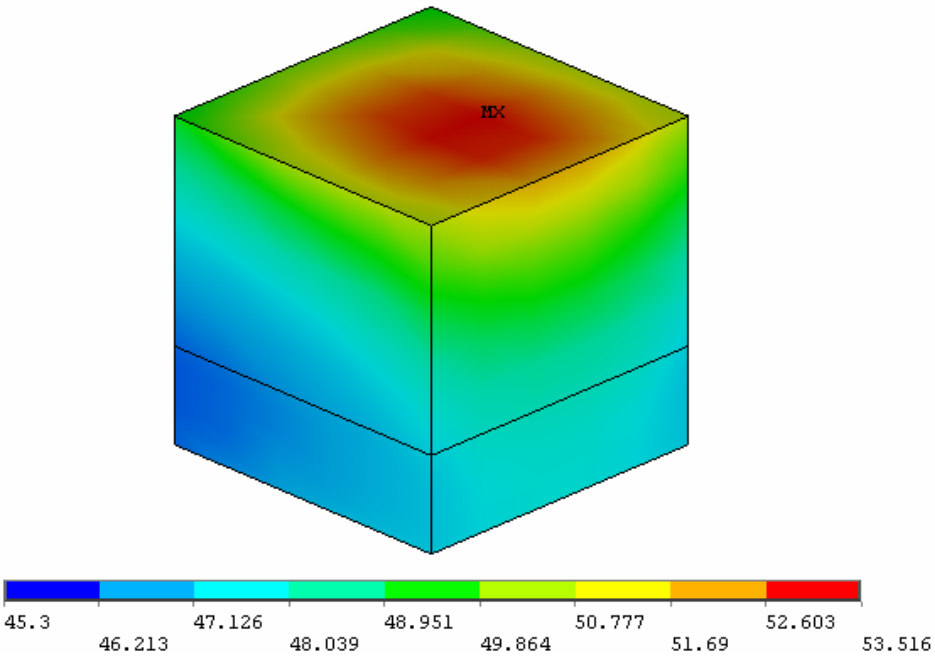

Figure 6-1 Temperature distribution in the Sun phase

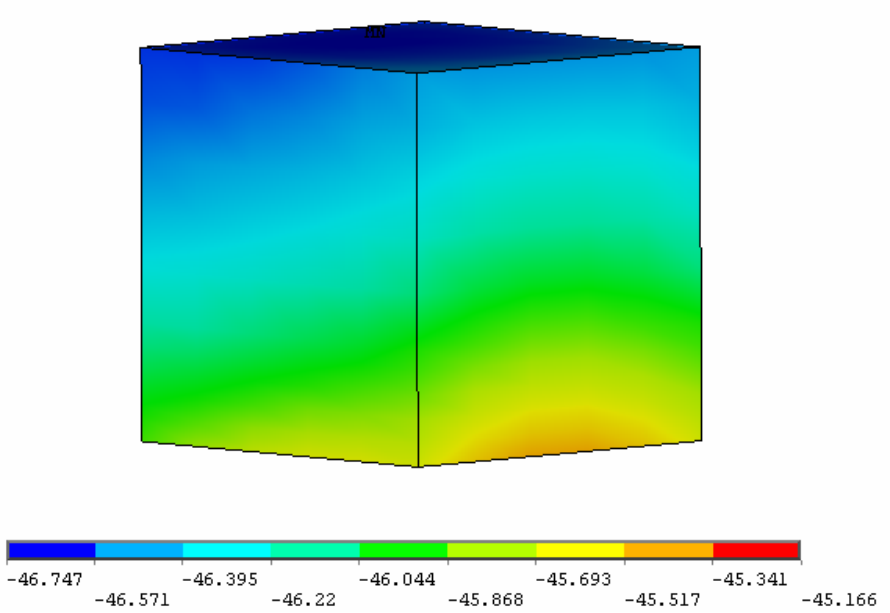

Figure 6-2 Temperature distribution in the eclipse

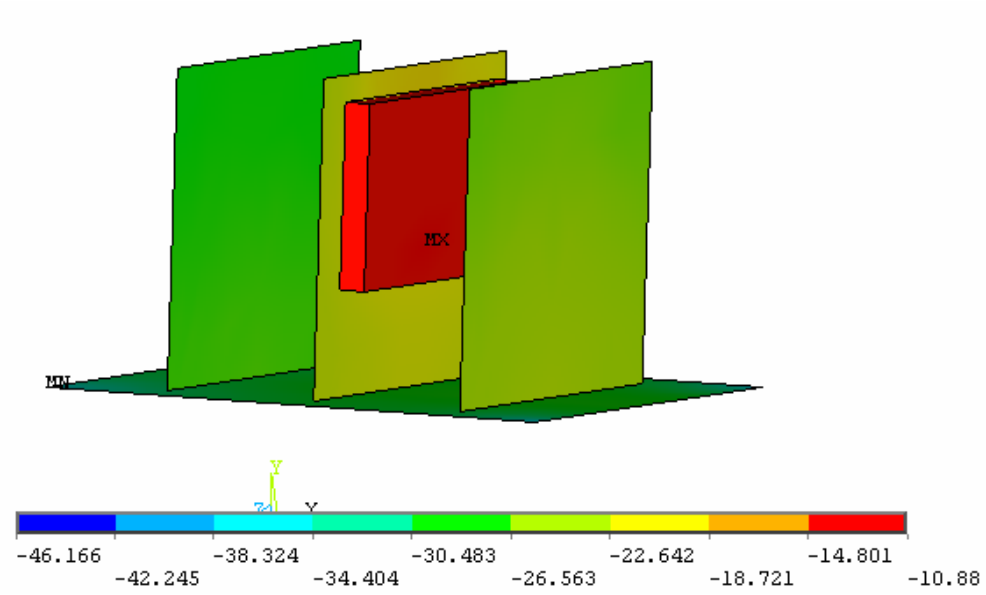

Figure 6-3 Temperature distribution inside Compass-1 in the eclipse

Appendix D

D.1 Heat Flow Fundamentals

Conduction and Convection
The first law of thermodynamics states that thermal energy is conserved. Specializing this to a differential control volume:

$$\rho c\left(\frac{\partial T}{\partial t}+\{v\}^T\{L\}T\right)+\{L\}^T\{q\}=\ddot{q} \qquad \text{(D.1)}$$

where:

ρ = density
c = specific heat
T = temperature (=T(x,y,z,t))
t = time

$$\{L\}=\begin{Bmatrix}\frac{\partial}{\partial x}\\ \frac{\partial}{\partial y}\\ \frac{\partial}{\partial z}\end{Bmatrix} = \text{vector operator}$$

$$\{v\}=\begin{Bmatrix}v_x\\ v_y\\ v_z\end{Bmatrix} = \text{velocity vector for mass transport of heat (input as VX, VY, VZ on } \mathbf{R} \text{ command, PLANE55 and SOLID70 only).}$$

{q} = heat flux vector

$\ddot{q}$ = heat generation rate per unit volume

It should be realized that the terms {L}T and $\{L\}^T\{q\}$ may also be interpreted as ∇T and $\nabla \cdot \{q\}$, respectively, where ∇ represents the grad operator and $\nabla \cdot$ represents the divergence operator. Next, Fourier's law is used to relate the heat flux vector to the thermal gradients:

$$\{q\} = -[D]\{L\}T \qquad \text{(D.2)}$$

where:

$$[D] = \begin{bmatrix} K_{xx} & 0 & 0 \\ 0 & K_{yy} & 0 \\ 0 & 0 & K_{zz} \end{bmatrix} = \text{conductivity matrix}$$

K_{xx}, K_{yy}, K_{zz} = conductivity in the element x, y, and z directions, respectively

Combining Equation (D.1) and Equation (D.2),

$$\rho c\left(\frac{\partial T}{\partial t} + \{v\}^T \{L\}T\right) = \{L\}^T([D]\{L\}T) + \ddot{q} \tag{D.3}$$

Expanding Equation D.3 to its more familiar form:

$$\rho c\left(\frac{\partial T}{\partial t} + v_x \frac{\partial T}{\partial x} + v_y \frac{\partial T}{\partial y} + v_z \frac{\partial T}{\partial z}\right) = \ddot{q} + \frac{\partial}{\partial x}\left(K_x \frac{\partial T}{\partial x}\right) + \frac{\partial}{\partial y}\left(K_y \frac{\partial T}{\partial y}\right) + \frac{\partial}{\partial z}\left(K_z \frac{\partial T}{\partial z}\right) \tag{D.4}$$

It will be assumed that all effects are in the global Cartesian system. Three types of boundary conditions are considered. It is presumed that these cover the entire element. Specified temperatures acting over surface S_1:

$$T = T^* \tag{D.5}$$

where T* is the specified temperature (input on D command).
Specified heat flows acting over surface S_2:

$$\{q\}^T\{\eta\} = -q^* \tag{D.6}$$

where:

{η} = unit outward normal vector
q* = specified heat flow

Specified convection surfaces acting over surface S_3 (Newton's law of cooling):

$$\{q\}^T\{\eta\} = h_f(T_S - T_B) \tag{D.7}$$

where:

h_f = film coefficient Evaluated at $(T_B + T_S)/2$ unless otherwise specified for the element

T_B = bulk temperature of the adjacent fluid

T_S = temperature at the surface of the model

Note that positive specified heat flow is into the boundary (i.e., in the direction opposite of {η}), which accounts for the negative signs in Equation (D.6) and Equation (D.7). Combining Equation (D.2) with Equation (D.6) and Equation (D.7)

$$\{\eta\}^T[D]\{L\}T = q^* \tag{D.8}$$

$$\{\eta\}^T[D]\{L\}T = h_f(T_B - T) \tag{D.9}$$

Premultiplying Equation (D.3) by a virtual change in temperature, integrating over the volume of the element, and combining with Equation (D.8) and Equation (D.9) with some manipulation yields:

$$\int_{vol}\left(\rho c\,\delta T\left(\frac{\partial T}{\partial t} + \{v\}^T\{L\}T\right) + \{L\}^T(\delta T)([D]\{L\}T)\right)d(vol) =$$
$$\int_{S_2}\delta T\,q^* d(S_2) + \int_{S_3}\delta T\,h_f(T_B - T)d(S_3) + \int_{vol}\delta T\,\ddot{q}\,d(vol) \tag{D.10}$$

where:

vol = volume of the element

δT = an allowable virtual temperature (=δT(x,y,z,t))

Radiation

Radiant energy exchange between neighboring surfaces of a region or between a region and its surroundings can produce large effects in the overall heat transfer problem. Though the radiation effects generally enter the heat transfer problem only through the boundary conditions, the coupling is especially strong due to nonlinear dependence of radiation on surface temperature.
Extending the Stefan-Boltzmann Law for a system of N enclosures, the energy balance for each surface in the enclosure for a gray diffuse body is given by Siegal and Howell [7], which relates the energy losses to the surface temperatures:

$$\sum_{i=1}^{N}\left(\frac{\delta_{ji}}{\varepsilon_i} - F_{ji}\frac{1-\varepsilon_i}{\varepsilon_i}\right)\frac{1}{A_i}Q_i = \sum_{i=1}^{N}(\delta_{ji} - F_{ji})\sigma T_i^4 \qquad \text{(D.11)}$$

where:

N = number of radiating surfaces
δ_{ij} = Kronecker delta
ε_i = effective emissivity of surface i
F_{ij} = radiation view factors (see below)
A_i = area of surface i
Q_i = energy loss of surface i
σ = Stefan-Boltzmann constant
T_i = absolute temperature of surface i

For a system of two surfaces radiating to each other, Equation (D.11) can be simplified to give the heat transfer rate between surfaces i and j as:

$$Q_i = \sigma\varepsilon_i F_{ij} A_i (T_i^4 - T_j^4) \qquad \text{(D.12)}$$

where:

T_i, T_j = absolute temperature at surface i and j, respectively

View Factors

The view factor, F_{ij}, is defined as the fraction of total radiant energy that leaves surface i which arrives directly on surface j, as shown in View Factor Calculation Terms. It can be expressed by the following equation:

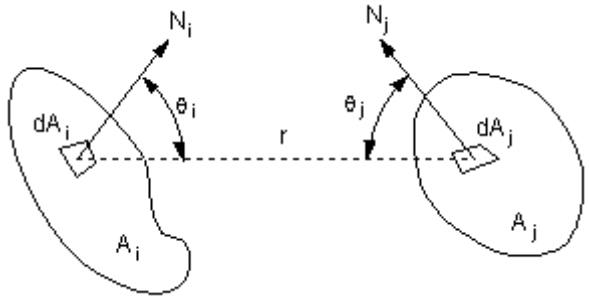

Figure D-1 View factor calculation terms

$$F_{ij} = \frac{1}{A_i} \int_{A_i} \int_{A_j} \frac{\cos\theta_i \cos\theta_j}{\pi r^2} d(A_j)\, d(A_i) \qquad \text{(D.13)}$$

where:

A_i, A_j = area of surface i and surface j
r = distance between differential surfaces i and j
θ_i = angle between N_i and the radius line to surface $d(A_j)$
θ_j = angle between N_j and the radius line to surface $d(A_i)$
N_i, N_j = surface normal of $d(A_i)$ and $d(A_j)$

D.2 Radiosity Solver Method

In the radiosity solver method for the analysis of gray diffuse radiation between N surfaces, Equation (D.11) is solved in conjunction with the basic conduction problem. For the purpose of computation it is convenient to rearrange Equation (D.11) into the following series of equations

$$\sum_{j=1}^{N} \left[\delta_{ij} - (1-\varepsilon_i) F_{ij} \right] q_j^o = \varepsilon_i \sigma T_i^4 \qquad \text{(D.14)}$$

and

$$q_i = q_i^o - \sum_{j=1}^{N} F_{ij} q_j^o \qquad \text{(D.15)}$$

Equation A38 and equation (D.15) are expressed in terms of the outgoing radiative fluxes (radiosity) for each surface, q_j^o, and the net flux from each surface q_i. For known surface temperatures, T_i, in the enclosure, equation (D.14) forms a set of linear algebraic equations for the unknown, outgoing radiative flux (radiosity) at each surface. Equation (D.14) can be written as

$$[A]\{q^o\} = \{D\} \qquad \text{(D.16)}$$

where:

$A_{ij} = \delta_{ij} - (1-\varepsilon_i)F_{ij}$

q_j^o = radiosity flux for surface i

$D_i = \varepsilon_i \sigma T_i^4$

[A] is a full matrix due to the surface to surface coupling represented by the view factors and is a function of temperature due to the possible dependence of surface emissivities on temperature. Equation (D.16) is solved using a Newton-Raphson procedure for the radiosity flux $\{q^o\}$.
When the q^o values are available, Equation (D.15) then allows the net flux at each surface to be evaluated. The net flux calculated during each iteration cycle is underrelaxed, before being updated using

$$q_i^{net} = \phi q_i^{k+1} + (1-\phi) q_i^k \qquad \text{(D.17)}$$

where:

φ = radiosity flux relaxation factor
k = iteration number

The net surface fluxes provide boundary conditions to the finite element model for the conduction process. The radiosity Equation (D.16) is solved coupled with the conduction Equation (D.11) using a segregated solution procedure until convergence of the radiosity flux and temperature for each time step or load step.
The surface temperatures used in the above computation must be uniform over each surface in order to satisfy conditions of the radiation model. In the finite element model, each surface in the radiation problem corresponds to a face or edge of a finite element. The uniform surface temperatures needed for use in Equation (D.16) are obtained by averaging the nodal point temperatures on the appropriate element face.
For open enclosure problems using the radiosity method, an ambient temperature needs to be specified using a space temperature or a space node, to account for energy balance between the radiating surfaces and the ambient.

View Factor Calculation - Hemicube Method
For solution of radiation problems in 3D, the radiosity method calculates the view factors using the hemicube method as compared to the traditional double area integration method for three-dimensional geometry. Details using the Hemicube method for view factor calculation are given in Glass [8] and Cohen and Greenberg [9]
The hemicube method is based upon Nusselt's hemisphere analogy. Nusselt's analogy shows that any surface, which covers the same area on the hemisphere, has the same view factor. From this it is evident that any intermediate surface geometry can be used without changing the value of the view factors. In the hemicube method, instead of projecting onto a sphere, an imaginary cube is constructed around the cen-

ter of the receiving patch. A patch in a finite element model corresponds to an element face of a radiating surface in an enclosure. The environment is transformed to set the center of the patch at the origin with the normal to the patch coinciding with the positive Z axis. In this orientation, the imaginary cube is the upper half of the surface of a cube, the lower half being below the 'horizon' of the patch. One full face is facing in the Z direction and four half faces are facing in the +X, -X, +Y, and -Y directions. These faces are divided into square 'pixels' at a given resolution, and the environment is then projected onto the five planar surfaces. The Hemicube shows the hemicube discretized over a receiving patch from the environment.
Figure D-2. The Hemicube

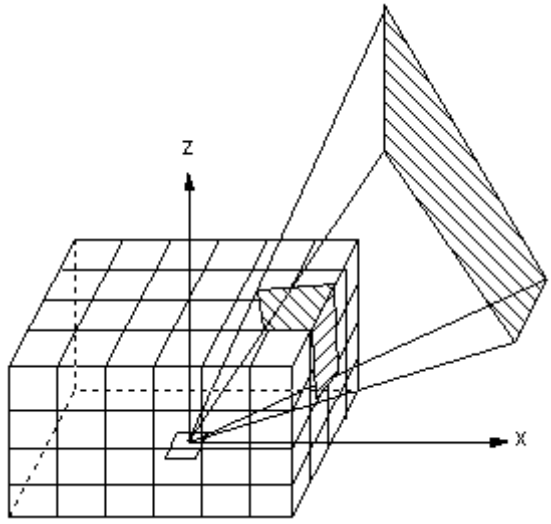

Figure D-2 Derivation of Delta-View Factors for Hemicube Method

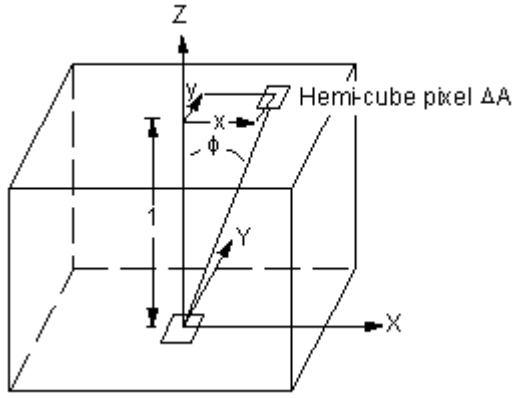

The contribution of each pixel on the cube's surface to the form-factor value varies and is dependent on the pixel location and orientation as shown in Derivation of Delta-View Factors for Hemicube Method. A specific delta form-factor value for each pixel on the cube is found from modified form of Equation (D.18) for the differential area to differential area form-factor. If two patches project on the same pixel on the cube, a depth determination is made as to which patch is seen in that particular direction by comparing distances to each patch and selecting the nearer one. After de-

termining which patch (j) is visible at each pixel on the hemicube, a summation of the delta form-factors for each pixel occupied by patch (j) determines the form-factor from patch (i) at the center of the cube to patch (j). This summation is performed for each patch (j) and a complete row of N form-factors is found.
At this point the hemicube is positioned around the center of another patch and the process is repeated for each patch in the environment. The result is a complete set of form-factors for complex environments containing occluded surfaces. The overall view factor for each surface on the hemicube is given by:

$$F_{ij} = \sum_{n=1}^{N} \Delta F_n = \frac{\cos\phi_i \cos\phi_j}{\pi r^2} \Delta A_j \qquad \text{(D.18)}$$

where:

N = number of pixels
ΔF = delta-view factor for each pixel

The hemicube resolution determines the accuracy of the view factor calculation and the speed at which they are calculated using the hemicube method. Default is set to 10. Higher values increase accuracy of the view factor calculation. [10]